Continuum Mech. Thermodyn. (2025) 37:5
https://doi.org/10.1007/s00161-024-01338-9

ORIGINAL ARTICLE

Anjuman · Manish Chopra · Subir Das · Holm Altenbach

Study of two-dimensional nonlinear coupled time-space fractional order reaction advection diffusion equations using shifted Legendre-Gauss-Lobatto collocation method

Received: 27 January 2024 / Accepted: 20 September 2024 / Published online: 23 November 2024

Abstract In this article, the nonlinear coupled two-dimensional space-time fractional order reaction-advection–diffusion equations (2D-STFRADEs) with initial and boundary conditions is solved by using Shifted Legendre-Gauss-Lobatto Collocation method (SLGLCM) with fractional derivative defined in Caputo sense. The SLGLC scheme is used to discretize the coupled nonlinear 2D-STFRADEs into the shifted Legendre polynomial roots to convert it to a system of algebraic equations. The efficiency and efficacy of the scheme are confirmed through error analysis while applying the scheme on two existing problems having exact solutions. The impact of advection and reaction terms on the solution profiles for various space and time fractional order derivatives are shown graphically for different particular cases. A drive has been made to study the convergence of the proposed scheme, which has been applied on the proposed mathematical model.

Keywords Two dimensional nonlinear coupled equations · Fractional order system · Reaction advection diffusion equations · Convergence analysis

1 Introduction

Water on earth is present in two forms - underground and surface water [1–3]. The majority of fresh water on Earth comes from underground sources, which account for around 97% of all fresh water. Groundwater system, also known as aquifer, is a porous media where the water is stored in the pore space within the soil grains. Sub-surface water is one of the purest forms of water due to its isolation from the biosphere. However, once contaminated, it is extremely expensive in terms of efforts and finances required to decontaminate it. Humans, wildlife, the ecosystem, etc., are all seriously harmed by polluted groundwater. The geological disposal of wastes of various kinds has become a probable hazard for the purity of groundwater. Hence, it is a regulatory requirement to demonstrate that such waste disposal does not harm the quality of groundwater up to an extent where it becomes unusable. The regulations require the analysis of impact of such waste disposal at different stages of the lifetime of the facility viz. siting, construction, operation, decommissioning, etc. The numerical

Anjuman · S. Das
Department of Mathematical Sciences, Indian Institute of Technology (BHU), Varanasi 221005, India
e-mail: anjuman.rs.mat21@itbhu.ac.in

S. Das
e-mail: sdas.apm@iitbhu.ac.in

M. Chopra
Radiation Safety Systems Division, Bhabha Atomic Research Centre, Mumbai 400085, India
e-mail: manish1307@gmail.com

H. Altenbach (✉)
Faculty of Mechanical Engineering, Otto von Guericke University Magdeburg, Universitätsplatz 2, Magdeburg 39106, Germany
e-mail: holm.altenbach@ovgu.de

modeling of transport of contaminants in groundwater is the most important tool for such impact assessment studies in the absence of measured values, especially in case of impact assessment at the siting or construction stages when facility is no longer existing. The nonlinear coupled 2D-STFRADEs have proven to be successful in describing the migration behaviour of conservative as well as non-conservative pollutants in groundwater [4,5]. These equations incorporate various physical phenomena such as advection, diffusion, molecular mixing, reaction, etc. In recent years, the significance of these equations in the mentioned field has led to enhanced interest of scientists and engineers in developing new and more efficient methods of their solution [6,7].

Using fractional calculus, it is possible to generalise integrals and derivatives of integer order to those of non-integer order. Various forms of fractional differential operators are introduced: Caputo type [8], Riemann-Liouville type [9], Grunwald-Letnikov type [10], etc. Fractional calculus has advanced significantly in recent years and attracted a lot of researchers in the fields of applied sciences, engineering, and economics [11–20]. The fractional order form of these equations is more important than the standard order for understanding many complex physical problems. Fractional-order forms of these equations are considered because there are many evidences that the standard-order equations cannot adequately describe most of the physical processes. The main advantage of the fractional differential operator is that it has both global and non-local properties, for instance, in dispersion phenomena to interpret the anomalous behavior of pollution in groundwater and porous soils.

In literature, numerous numerical methods for solving space-time fractional reaction-advection–diffusion equations are available, among them are the Shifted Legendre Collocation scheme [21], Chebyshev wavelets collocation method [22], Finite element method [23], Finite difference method [24], Neural network method [25], Shifted Jacobi collocation method [26]. Ren et al. [27] have found a numerical scheme for solving the space fractional diffusion equation based on the shifted Chebyshev-tau algorithm [28]. The two dimension fractional diffusion equation have been solved numerically, using the finite difference method [29,30] and the Fourier spectral technique [31]. Hadhoud [32] suggested that the time fractional Burgers' nonlinear coupled equations can be solved numerically using the Non-polynomial B-spline [33] and Shifted Jacobi spectral collocation [34] techniques. A class of fractional reaction-diffusion models are solved numerically in [35]. Zhang et al. [36] have suggested that the two-dimensional nonlinear fractional diffusion-wave equations can be solved using a second-order stabilized semi-implicit time-stepping Fourier spectral method [37]. The numerical solution for a class of multi term variable-order fractional differential equations has been obtained using shifted Legendre polynomials [38]. Two shifted Jacobi-Gauss collocation schemes [39] are used for solving two-dimensional variable-order fractional Rayleigh-Stokes problem and variable fractional order equation [40,41]. Space and time fractional order coupled reaction diffusion equations in two dimensions are solved using the SLGLCM [42]. Here it is specified that in the model the advection terms have not been considered by the authors. Moreover there were a scope of showing the effect of nonlinear reaction terms on the solution profile.

In the classical mechanics, the interaction between two objects is known as coupling. For the coupled diffusion process the concentration of one system affects the concentration of the other system. In other words, we can say that the effect of the macroscopic behaviors of micro-particles of one system on the other system due to the Brownian motions of the particles, is known as coupled reaction-advection–diffusion equations. Therefore, in the present article the authors have made an endeavour to solve a two-dimensional nonlinear coupled space-time fractional order reaction-advection-diffusion equations given by

$$\begin{aligned}\frac{\partial^{\gamma}\tilde{u}(x,y,t)}{\partial t^{\gamma}} &= \frac{\partial^{1+\alpha}\tilde{u}(x,y,t)}{\partial x^{1+\alpha}} + \frac{\partial^{1+\beta}\tilde{u}(x,y,t)}{\partial y^{1+\beta}} + \nu_1\frac{\partial^{\alpha}\tilde{u}(x,y,t)}{\partial x^{\alpha}} \\ &\quad +\lambda_1\,\tilde{u}(x,y,t)\left(\tilde{u}(x,y,t)-\tilde{v}(x,y,t)\right)+g_1(x,y,t), \qquad (1)\\ \frac{\partial^{\gamma}\tilde{v}(x,y,t)}{\partial t^{\gamma}} &= \frac{\partial^{1+\alpha}\tilde{v}(x,y,t)}{\partial x^{1+\alpha}} + \frac{\partial^{1+\beta}\tilde{v}(x,y,t)}{\partial y^{1+\beta}} + \nu_2\frac{\partial^{\beta}\tilde{v}(x,y,t)}{\partial y^{\beta}} \\ &\quad +\lambda_2\,\tilde{v}(x,y,t)\left(\tilde{v}(x,y,t)-\tilde{u}(x,y,t)\right)+g_2(x,y,t), \qquad (2)\end{aligned}$$

under the initial and boundary conditions as

$$\left.\begin{array}{ll}\tilde{u}(x,y,0)=h_1(x,y), & \tilde{u}(0,y,t)=h_2(y,t)\\ \tilde{u}(X,y,t)=h_3(y,t), & \tilde{u}(x,0,t)=h_4(x,t)\\ \tilde{u}(x,Y,t)=h_5(x,t), & \tilde{v}(x,y,0)=h_6(x,y)\\ \tilde{v}(0,y,t)=h_7(y,t), & \tilde{v}(X,y,t)=h_8(y,t)\\ \tilde{v}(x,0,t)=h_9(x,t), & \tilde{v}(x,Y,t)=h_{10}(x,t)\end{array}\right\} \qquad (3)$$

where $0 \le x \le X,\ 0 \le y \le Y,\ 0 \le t \le T,\ 0 < \gamma \le 1,\ 0 < \alpha \le 1,\ 0 < \beta \le 1,\ \nu_1, \nu_2$ are the advection coefficients, $\lambda_1,\ \lambda_2$ are the reaction coefficients and $g_1(x, y, t), g_2(x, y, t)$ are the force functions. $h_1(x, y)$, $h_2(y, t), h_3(y, t), h_4(x, t), h_5(x, t), h_6(x, y), h_7(y, t), h_8(y, t), h_9(x, t), h_{10}(x, t)$ are sufficiently smooth functions. The salient feature of the article is the graphical presentations of the effect of concentration of one system on the other in the fractional order system for different particular cases.

The remaining sections of the article are organised as follows: Sect. 2 introduces a few useful definitions and properties which are utilized in the development of numerical solution. In Sect. 3 the proposed numerical scheme is provided in detail which is used to solve the nonlinear coupled 2D-STFRAD by converting those into a system of algebraic equations, which are solved using the Newton-Cotes method [43]. The error and convergence analyses are furnished in Sect. 4. Two test problems are given in Sect. 5 to validate the efficiency of the proposed numerical scheme. The concerned coupled fractional order model is solved using the proposed scheme in Sect. 6, which is followed by a overall conclusion of the present research given in Sect. 7.

2 Preliminaries

Some basic theories and properties are introduced in this section. They have been used to solve the considered 2D-STFRADEs in the later sections.

2.1 Caputo fractional derivative

Caputo fractional α order derivative of a function $\tilde{u}(x, y, t)$ with respect to t is given as [44]

$$ {}_0^cD_t^\alpha \tilde{u}(x, y, t) = \begin{cases} \dfrac{1}{\Gamma(n-\alpha)} \displaystyle\int_0^t \dfrac{1}{(t-\tau)^{\alpha-n+1}} \dfrac{\partial^n \tilde{u}(x, y, \tau)}{\partial \tau^n} \mathrm{d}\tau, & \text{if } n-1 < \alpha < n \in \mathbb{N}, \\ \dfrac{\partial^n \tilde{u}(x, y, t)}{\partial t^n}, & \text{if } \alpha = n \in \mathbb{N}. \end{cases} \tag{4}$$

Caputo fractional derivative satisfies linearity property, i.e., ${}_0^cD_t^\alpha(\mu_1\, \tilde{u} + \mu_2\, \tilde{v}) = \mu_1\, {}_0^cD_t^\alpha \tilde{u} + \mu_2\, {}_0^cD_t^\alpha \tilde{v}$ where μ_1, μ_2 are constants.

2.2 Legendre polynomial

In this section, some important properties of shifted Legendre polynomial have been introduced. It is assumed that $P_k(z)$ represents the kth degree Legendre polynomial (in the interval $[-1, 1]$) as given in [42]. Then $P_k(z)$ satisfies recurrence relation

$$P_{k+1}(z) = \frac{2k+1}{k+1} z P_k(z) - \frac{k}{k+1} P_{k-1}(z), \quad k = 1, 2, 3, ...$$

where $P_0(z) = 1,\quad P_1(z) = z$.

Introducing $z = \frac{2z}{Z} - 1$, a shifted Legendre polynomial in the interval $[0, Z]$. The shifted Legendre polynomials $P_{Z,k}(z)$ are produced by using the recurrence formulas

$$P_{Z,k}(z) = \frac{2k+1}{k+1}\left(\frac{2z-Z}{Z}\right) P_{Z,k}(z) - \frac{k}{k+1} P_{Z,k-1}(z), \quad k = 1, 2, 3, ...;$$
$$P_{Z,0}(z) = 1,\ P_{Z,1}(z) = \frac{2z}{Z} - 1$$

which satisfy the orthogonality property

$$\begin{cases} \displaystyle\int_0^Z P_{Z,i}(z) P_{Z,k}(z) \mathrm{d}z = \dfrac{Z}{2k+1}, & \text{for } i = k, \\ \qquad\qquad\qquad\qquad\quad = 0, & \text{for } i \ne k. \end{cases}$$

An explicit analytical form of the shifted Legendre polynomial is

$$P_{Z,k}(z) = \sum_{s=0}^{k} \frac{(k+s)! z^s}{(k-s)!(s!)^2 Z^s}.$$

3 Shifted Legendre-Gauss-Lobatto collocation method

In this section, an attempt is made to use the efficient and effective method SLGLCM [42] consisting of Legendre polynomials to solve the 2D-nonlinear coupled space-time fractional order reaction-advection–diffusion Eqs. (1) and (2) under the prescribed initial and boundary condition.

The approximate solutions for 2D-STFRAD nonlinear coupled equations are defined as

$$\tilde{u}(x,y,t) \simeq \sum_{i=0}^{N_x}\sum_{j=0}^{M_y}\sum_{k=0}^{K_t} \check{c}_{i,j,k} P_{T,k}(t) P_{X,i}(x) P_{Y,j}(y), \tag{5}$$

$$\tilde{v}(x,y,t) \simeq \sum_{i=0}^{N_x}\sum_{j=0}^{M_y}\sum_{k=0}^{K_t} \check{d}_{i,j,k} P_{T,k}(t) P_{X,i}(x) P_{Y,j}(y), \tag{6}$$

where $P_{T,k}(t)$, $P_{X,i}(x)$ and $P_{Y,j}(y)$ are the shifted Legendre Polynomials given in the Sect. 2.2, N_x, M_y and K_t are positive integers. Therefore, the unknowns $\check{c}_{i,j,k}$, $\check{d}_{i,j,k}$ and hence, the concentrations $\tilde{u}(x,y,t)$, $\tilde{v}(x,y,t)$ are obtained by substituting (5) and (6) into Eqs. (1) and (2), and satisfying Eqs. (3).

To calculate the standard and Caputo fractional order derivatives of basis functions $P_{T,k}(t)$, $P_{X,i}(x)$ and $P_{Y,j}(y)$, let us consider

$$T(t) = [P_{T,0}(t), P_{T,1}(t), ..., P_{T,K_t}(t)],$$

where $P_{T,k}(t) = \sum_{s=0}^{k} (-1)^{(k+s)} \dfrac{(k+s)!t^s}{(k-s)!(s!)^2 T^s}, \quad k = 0, 1, 2, ...;$

Case 1: for $\gamma = 1$, we have

$$\frac{\mathrm{d}T(t)}{\mathrm{d}t} = \frac{\mathrm{d}}{\mathrm{d}t}[P_{T,0}(t), P_{T,1}(t), ..., P_{T,K_t}(t)] = [0, P'_{T,1}(t), ..., P'_{T,K_t}(t)], \tag{7}$$

where $P'_{T,k}(t) = \sum_{s=1}^{k} (-1)^{(k+s)} \dfrac{(k+s)!t^{(s-1)}}{(k-s)!(s!)(s-1)!T^s}, \quad k = 1, 2, 3, ...$

Case 2:

$${}_0^cD_t^\gamma T(t) = [0, P^\gamma_{T,1}(t), ..., P^\gamma_{T,K_t}(t)], \quad \gamma \in (0,1), \tag{8}$$

where

$${}_0^cD_t^\gamma P_{T,k}(t) = \sum_{s=1}^{k} (-1)^{(k+s)} \frac{(k+s)!t^{s-\gamma}}{(k-s)!(s!)\Gamma(k+1-\gamma)T^s}. \tag{9}$$

To calculate the spatial derivatives for x, let us consider

$$P(x) = [P_{X,0}(x), P_{X,1}(x), ..., P_{X,N_x}(x)].$$

For second order derivative of $P_{X,i}(x)$, consider

$$\frac{\mathrm{d}^2X(x)}{\mathrm{d}x^2} = \frac{\mathrm{d}^2}{\mathrm{d}x^2}[P_{X,0}(x), P_{X,1}(x), ..., P_{X,N_x}(x)] = [0, P''_{X,1}(x), ..., P''_{X,N_x}(x)], \tag{10}$$

where

$$P''_{X,i}(x) = \sum_{s=2}^{i}(-1)^{(i+s)} \frac{(i+s)!x^{(s-2)}}{(i-s)!(s!)(s-2)!X^s}, \quad i = 2, 3, 4, ...$$

Now

$${}_0^cD_x^\alpha X(x) = [0, P^\alpha_{X,1}(x), ..., P^\alpha_{X,N_x}(x)], \quad \alpha \in (0,1), \tag{11}$$

where

$$ {}_{0}^{c}D_{x}^{\alpha} P_{X,i}(x) = \sum_{s=1}^{i} (-1)^{(i+s)} \frac{(i+s)!x^{s-\alpha}}{(i-s)!(s!)\Gamma(s+1-\alpha)X^{s}}. \tag{12} $$

Similarly for spatial derivative for y, the second order derivative of $P_{Y,j}(y)$ is

$$ \frac{\mathrm{d}^2 Y(y)}{\mathrm{d}y^2} = \frac{\mathrm{d}^2}{\mathrm{d}y^2}[P_{Y,0}(y), P_{Y,1}(y), ..., P_{Y,M_y}(y)] = [0, P''_{Y,1}(y), ..., P''_{Y,M_y}(y)], \tag{13} $$

where $P''_{Y,j}(y) = \sum_{s=2}^{j} (-1)^{(j+s)} \frac{(j+s)!y^{(s-2)}}{(j-s)!(s!)(s-2)!Y^{s}}, \quad j = 2, 3, 4, ...;$

For $\beta \in (0, 1)$, we have

$$ {}_{0}^{c}D_{y}^{\beta} Y(y) = [0, P^{\beta}_{Y,1}(y), ..., P^{\beta}_{Y,M_y}(y)], \tag{14} $$

where

$$ {}_{0}^{c}D_{y}^{\beta} P_{Y,j}(y) = \sum_{s=1}^{j} (-1)^{(j+s)} \frac{(j+s)!y^{s-\beta}}{(j-s)!(s!)\Gamma(s+1-\beta)Y^{s}}. \tag{15} $$

The fractional derivatives at the SLGL nodes $x_{N_x,\mathbf{p}}$, $y_{M_y,\mathbf{q}}$ and $t_{K_t,\mathbf{r}}$ are calculated as

$$ \left.\frac{\partial^{\alpha}\tilde{u}(x, y_{M_y,\mathbf{q}}, t_{K_t,\mathbf{r}})}{\partial x^{\alpha}}\right|_{x=x_{N_x,\mathbf{p}}} \simeq \sum_{i=0}^{N_x}\sum_{j=0}^{M_y}\sum_{k=0}^{K_t} \check{c}_{i,j,k} P_{T,k}(t_{K_t,\mathbf{r}})\, {}_{0}^{c}D_{x}^{\alpha} P_{X,i}(x)\big|_{x=x_{N_x,\mathbf{p}}} P_{Y,j}(y_{M_y,\mathbf{q}}), \tag{16} $$

$$ \left.\frac{\partial^{\beta}\tilde{u}(x_{N_x,\mathbf{p}}, y, t_{K_t,\mathbf{r}})}{\partial y^{\beta}}\right|_{y=y_{M_y,\mathbf{q}}} \simeq \sum_{i=0}^{N_x}\sum_{j=0}^{M_y}\sum_{k=0}^{K_t} \check{c}_{i,j,k} P_{T,k}(t_{K_t,\mathbf{r}}) P_{X,i}(x_{N_x,\mathbf{p}})\, {}_{0}^{c}D_{y}^{\beta} P_{Y,j}(y)\big|_{y=y_{M_y,\mathbf{q}}}, \tag{17} $$

$$ \left.\frac{\partial^{\gamma}\tilde{u}(x_{N_x,\mathbf{p}}, y_{M_y,\mathbf{q}}, t)}{\partial t^{\gamma}}\right|_{t=t_{K_t,\mathbf{r}}} \simeq \sum_{i=0}^{N_x}\sum_{j=0}^{M_y}\sum_{k=0}^{K_t} \check{c}_{i,j,k}\, {}_{0}^{c}D_{t}^{\gamma} P_{T,k}(t)\big|_{t=t_{K_t,\mathbf{r}}} P_{X,i}(x_{N_x,\mathbf{p}}) P_{Y,j}(y_{M_y,\mathbf{q}}), \tag{18} $$

$$ \left.\frac{\partial^{\alpha}\tilde{v}(x, y_{M_y,\mathbf{q}}, t_{K_t,\mathbf{r}})}{\partial x^{\alpha}}\right|_{x=x_{N_x,\mathbf{p}}} \simeq \sum_{i=0}^{N_x}\sum_{j=0}^{M_y}\sum_{k=0}^{K_t} \check{d}_{i,j,k} P_{T,k}(t_{K_t,\mathbf{r}})\, {}_{0}^{c}D_{x}^{\alpha} P_{X,i}(x)\big|_{x=x_{N_x,\mathbf{p}}} P_{Y,j}(y_{M_y,\mathbf{q}}), \tag{19} $$

$$ \left.\frac{\partial^{\beta}\tilde{v}(x_{N_x,\mathbf{p}}, y, t_{K_t,\mathbf{r}})}{\partial y^{\beta}}\right|_{y=y_{M_y,\mathbf{p}}} \simeq \sum_{i=0}^{N_x}\sum_{j=0}^{M_y}\sum_{k=0}^{K_t} \check{d}_{i,j,k} P_{T,k}(t_{K_t,\mathbf{r}}) P_{X,i}(x_{N_x,\mathbf{p}})\, {}_{0}^{c}D_{y}^{\beta} P_{Y,j}(y)\big|_{y=y_{M_y,\mathbf{q}}}, \tag{20} $$

$$ \left.\frac{\partial^{\gamma}\tilde{v}(x_{N_x,\mathbf{p}}, y_{M_y,\mathbf{q}}, t)}{\partial t^{\gamma}}\right|_{t=t_{K_t,\mathbf{r}}} \simeq \sum_{i=0}^{N_x}\sum_{j=0}^{M_y}\sum_{k=0}^{K_t} \check{d}_{i,j,k}\, {}_{0}^{c}D_{t}^{\gamma} P_{T,k}(t)\big|_{t=t_{K_t,\mathbf{r}}} P_{X,i}(x_{N_x,\mathbf{p}}) P_{Y,j}(y_{M_y,\mathbf{q}}). \tag{21} $$

The aim of this scheme is to estimate the residuals from Eqs. (1) and (2) which are set to zero at

$$ 2(N_x - 1)(M_y - 1)K_t $$

collocation points. So, substituting all these Eqs. (5), (6) and (16)–(21) in Eqs. (1) and (2), we get

$$ \sum_{i=0}^{N_x}\sum_{j=0}^{M_y}\sum_{k=0}^{K_t} \check{c}_{i,j,k}\phi_{1_{i,j,k}} - \lambda_1\, G_1(\tilde{u}_{\mathbf{p},\mathbf{q},\mathbf{r}}, \tilde{v}_{\mathbf{p},\mathbf{q},\mathbf{r}}) - g_{1_{\mathbf{p},\mathbf{q},\mathbf{r}}} = 0\,, \tag{22} $$

$$ \sum_{i=0}^{N_x}\sum_{j=0}^{M_y}\sum_{k=0}^{K_t} \check{d}_{i,j,k}\phi_{2_{i,j,k}} - \lambda_2\, G_2(\tilde{u}_{\mathbf{p},\mathbf{q},\mathbf{r}}, \tilde{v}_{\mathbf{p},\mathbf{q},\mathbf{r}}) - g_{2_{\mathbf{p},\mathbf{q},\mathbf{r}}} = 0, \tag{23} $$

where $\mathbf{p} = 1, 2, 3, ..., N_x - 1$, $\mathbf{q} = 1, 2, 3, ..., M_y - 1$, $\mathbf{r} = 1, 2, 3, ..., K_t$ and

$$\begin{aligned}
&\tilde{u}_{\mathbf{p},\mathbf{q},\mathbf{r}} = \tilde{u}(x_{N_x,\mathbf{p}}, y_{M_y,\mathbf{q}}, t_{K_t,\mathbf{r}}),\\
&\tilde{v}_{\mathbf{p},\mathbf{q},\mathbf{r}} = \tilde{v}(x_{N_x,\mathbf{p}}, y_{M_y,\mathbf{q}}, t_{K_t,\mathbf{r}}),\\
&G_1(\tilde{u}_{\mathbf{p},\mathbf{q},\mathbf{r}}, \tilde{v}_{\mathbf{p},\mathbf{q},\mathbf{r}}) = \tilde{u}^2(x_{N_x,\mathbf{p}}, y_{M_y,\mathbf{q}}, t_{K_t,\mathbf{r}}) - \tilde{u}(x_{N_x,\mathbf{p}}, y_{M_y,\mathbf{q}}, t_{K_t,\mathbf{r}}) \times \tilde{v}(x_{N_x,\mathbf{p}}, y_{M_y,\mathbf{q}}, t_{K_t,\mathbf{r}}),\\
&G_2(\tilde{u}_{\mathbf{p},\mathbf{q},\mathbf{r}}, \tilde{v}_{\mathbf{p},\mathbf{q},\mathbf{r}}) = \tilde{v}^2(x_{N_x,\mathbf{p}}, y_{M_y,\mathbf{q}}, t_{K_t,\mathbf{r}}) - \tilde{u}(x_{N_x,\mathbf{p}}, y_{M_y,\mathbf{q}}, t_{K_t,\mathbf{r}}) \times \tilde{v}(x_{N_x,\mathbf{p}}, y_{M_y,\mathbf{q}}, t_{K_t,\mathbf{r}}),\\
&g_{1_{\mathbf{p},\mathbf{q},\mathbf{r}}} = g_1(x_{N_x,\mathbf{p}}, y_{M_y,\mathbf{q}}, t_{K_t,\mathbf{r}}),\\
&g_{2_{\mathbf{n},\mathbf{m},\mathbf{r}}} = g_2(x_{N_x,\mathbf{p}}, y_{M_y,\mathbf{q}}, t_{K_t,\mathbf{r}}),\\
&\phi_{1_{i,j,k}} = {}_0^cD_t^{\gamma} P_{T,k}(t)\big|_{t=t_{K_t,k}} P_{X,i}(x_{N_x,\mathbf{p}}) P_{Y,j}(y_{M_y,\mathbf{q}}) - P_{T,k}(t_{K_t,\mathbf{r}}) {}_0^cD_x^{1+\alpha} P_{X,i}(x)\big|_{x=x_{N_x,\mathbf{q}}} P_{Y,j}(y_{M_y,\mathbf{q}})\\
&\qquad - P_{T,k}(t_{K_t,\mathbf{r}}) P_{X,i}(x_{N_x,\mathbf{p}}) {}_0^cD_y^{1+\beta} P_{Y,j}(y)\big|_{y=y_{M_y,\mathbf{q}}} - \nu_1 P_{T,k}(t_{K_t,\mathbf{r}})\, {}_0^cD_x^{\alpha} P_{X,i}(x)\big|_{x=x_{N_x,\mathbf{p}}} P_{Y,j}(y_{M_y,\mathbf{q}}),\\
&\phi_{2_{i,j,k}} = {}_0^cD_t^{\gamma} P_{T,k}(t)\big|_{t=t_{K_t,\mathbf{r}}} P_{X,i}(x_{N_x,\mathbf{p}}) P_{Y,j}(y_{M_y,\mathbf{q}}) - P_{T,k}(t_{K_t,\mathbf{r}})\, {}_0^cD_x^{1+\alpha} P_{X,i}(x)\big|_{x=x_{N_x,\mathbf{p}}} P_{Y,j}(y_{M_y,\mathbf{q}})\\
&\qquad - P_{T,k}(t_{K_t,\mathbf{r}}) P_{X,i}(x_{N_x,\mathbf{p}})\, {}_0^cD_y^{1+\beta} P_{Y,j}(y)\big|_{y=y_{M_y,\mathbf{q}}} - \nu_2 P_{T,k}(t_{K_t,\mathbf{r}}) P_{X,i}(x_{N_x,\mathbf{p}})\, {}_0^cD_y^{\beta} P_{Y,j}(y)\big|_{y=y_{M_y,\mathbf{q}}}.
\end{aligned}$$

The above system consists of $2(N_x - 1)(M_y - 1)K_t$ equations with $2(N_x + 1)(M_y + 1)(K_t + 1)$ unknown coefficients. To find the unique solution of the above system we require

$$2\big(1 + M_y + N_x + N_x M_y + 2K_t(N_x + M_y)\big)$$

additional equations. Again $2\big(1 + M_y + N_x + N_x M_y + 2K_t(N_x + M_y)\big)$ additional equations are derived from the initial and boundary conditions.

$$\sum_{i=0}^{N_x} \sum_{j=0}^{M_y} \sum_{k=0}^{K_t} \check{c}_{i,j,k} P_{T,k}(0) P_{X,i}(x_{N_x,\mathbf{p}}) P_{Y,j}(y_{M_y,\mathbf{p}}) = h_{1_{\mathbf{p},\mathbf{q}}},$$

$$\sum_{i=0}^{N_x} \sum_{j=0}^{M_y} \sum_{k=0}^{K_t} \check{d}_{i,j,k} P_{T,k}(0) P_{X,i}(x_{N_x,\mathbf{p}}) P_{Y,j}(y_{M_y,\mathbf{q}}) = h_{6_{\mathbf{p},\mathbf{q}}},$$

where $\mathbf{p} = 1, 2, 3, ..., N_x - 1$, $\mathbf{q} = 1, 2, 3, ..., M_y - 1$.

$$\sum_{i=0}^{N_x} \sum_{j=0}^{M_y} \sum_{k=0}^{K_t} \check{c}_{i,j,k} P_{T,k}(t_{K_t,\mathbf{r}}) P_{X,i}(0) P_{Y,j}(y_{M_y,\mathbf{q}}) = h_{2_{\mathbf{q},\mathbf{r}}},$$

$$\sum_{i=0}^{N_x} \sum_{j=0}^{M_y} \sum_{k=0}^{K_t} \check{d}_{i,j,k} P_{T,k}(t_{K_t,\mathbf{r}}) P_{X,i}(0) P_{Y,j}(y_{M_y,\mathbf{q}}) = h_{7_{\mathbf{q},\mathbf{r}}},$$

$$\sum_{i=0}^{N_x} \sum_{j=0}^{M_y} \sum_{k=0}^{K_t} \check{c}_{i,j,k} P_{T,k}(t_{K_t,\mathbf{r}}) P_{X,i}(X) P_{Y,j}(y_{M_y,\mathbf{q}}) = h_{3_{\mathbf{q},\mathbf{r}}},$$

$$\sum_{i=0}^{N_x} \sum_{j=0}^{M_y} \sum_{k=0}^{K_t} \check{d}_{i,j,k} P_{T,k}(t_{K_t,\mathbf{r}}) P_{X,i}(X) P_{Y,j}(y_{M_y,\mathbf{q}}) = h_{8_{\mathbf{q},\mathbf{r}}},$$

where $\mathbf{q} = 0, 1, 2, ..., M_y$, $\mathbf{r} = 0, 1, 2, ..., K_t$.

$$\sum_{i=0}^{N_x}\sum_{j=0}^{M_y}\sum_{k=0}^{K_t} \check{c}_{i,j,k} P_{T,k}(t_{K_t,\mathbf{r}}) P_{X,i}(x_{N_x,\mathbf{p}}) P_{Y,j}(0) = h_{4_{\mathbf{p},\mathbf{r}}},$$

$$\sum_{i=0}^{N_x}\sum_{j=0}^{M_y}\sum_{k=0}^{K_t} \check{d}_{i,j,k} P_{T,k}(t_{K_t,\mathbf{r}}) P_{X,i}(x_{N_x,\mathbf{p}}) P_{Y,j}(0) = h_{9_{\mathbf{p},\mathbf{r}}},$$

$$\sum_{i=0}^{N_x}\sum_{j=0}^{M_y}\sum_{k=0}^{K_t} \check{c}_{i,j,k} P_{T,k}(t_{K_t,\mathbf{r}}) P_{X,i}(x_{N_x,\mathbf{p}}) P_{Y,j}(Y) = h_{5_{\mathbf{p},\mathbf{r}}},$$

$$\sum_{i=0}^{N_x}\sum_{j=0}^{M_y}\sum_{k=0}^{K_t} \check{d}_{i,j,k} P_{T,k}(t_{K_t,\mathbf{r}}) P_{X,i}(x_{N_x,\mathbf{p}}) P_{Y,j}(Y) = h_{10_{\mathbf{p},\mathbf{r}}},$$

where $\mathbf{p} = 1, 2, 3, ..., N_x - 1$, $\mathbf{r} = 0, 1, 2, ..., K_t$.

Hence, for $h_{i_{\mathbf{p},\mathbf{q}}} = h_i(x_{N_x,\mathbf{p}},\ y_{M_y,\mathbf{q}})$, $i = 1, 6$, $h_{j_{\mathbf{q},\mathbf{r}}} = h_j(y_{M_y,\mathbf{q}},\ t_{K_t,\mathbf{r}})$, $j = 2, 3, 7, 8$ and $h_{k_{\mathbf{p},\mathbf{r}}} = h_k(x_{N_x,\mathbf{p}},\ t_{K_t,\mathbf{r}})$, $k = 4, 5, 9, 10$, we obtain a system of $2(N_x + 1)(M_y + 1)(K_t + 1)$ algebraic equations with $2(N_x + 1)(M_y + 1)(K_t + 1)$ unknown coefficients, which can be easily solved. After finding the coefficients, one may determine the solutions of $\tilde{u}(x, y, t)$ and $\tilde{v}(x, y, t)$ from the expressions (5) and (6).

4 Error and convergence analyses

In this Section the attempt is made to estimate the error bounds and analyse the convergence of the solutions. Let $\tilde{u}(x, y, t)$ and $\tilde{v}(x, y, t)$ be sufficiently smooth functions in the domain $[0, X] \times [0, Y] \times [0, T]$.

Theorem 1 [42] *Let us consider $\tilde{U}_{\mathcal{N}_x,\mathcal{M}_y,K_t}(x, y, t)$ and $\tilde{V}_{\mathcal{N}_x,\mathcal{M}_y,K_t}(x, y, t)$ are the best approximations of functions $\tilde{u}(x, y, t)$ and $\tilde{v}(x, y, t)$, respectively. Then, we have*

$$||\tilde{u}(x, y, t) - \tilde{U}_{N_x,M_y,K_t}(x, y, t)||_{L_2} \le (XYT)^{\frac{1}{2}} A_1 \left(\frac{1}{4}\left(\frac{X}{N_x}\right)^{N_x+1} + \frac{1}{4}\left(\frac{Y}{M_y}\right)^{M_y+1} + \frac{1}{4}\left(\frac{T}{K_t}\right)^{K_t+1} + \frac{1}{64}\left(\frac{X}{N_x}\right)^{N_x+1}\left(\frac{Y}{M_y}\right)^{M_y+1}\left(\frac{T}{K_t}\right)^{K_t+1}\right), \tag{24}$$

$$||\tilde{v}(x, y, t) - \tilde{V}_{N_x,M_y,K_t}(x, y, t)||_{L_2} \le (XYT)^{\frac{1}{2}} A_2 \left(\frac{1}{4}\left(\frac{X}{N_x}\right)^{N_x+1} + \frac{1}{4}\left(\frac{Y}{M_y}\right)^{M_y+1} + \frac{1}{4}\left(\frac{T}{K_t}\right)^{K_t+1} + \frac{1}{64}\left(\frac{X}{N_x}\right)^{N_x+1}\left(\frac{Y}{M_y}\right)^{M_y+1}\left(\frac{T}{K_t}\right)^{K_t+1}\right), \tag{25}$$

where $\mathcal{A}_1$ and $\mathcal{A}_2$ are given in Appendix A.

Theorem 2 [42] *Consider $\tilde{U}_{\mathcal{N}_x,\mathcal{M}_y,K_t}(x, y, t) = \sum_{i=0}^{N_x}\sum_{j=0}^{M_y}\sum_{k=0}^{K_t} \bar{c}_{i,j,k} P_{T,k}(t) P_{X,i}(x) P_{Y,j}(y)$ and $\tilde{V}_{\mathcal{N}_x,\mathcal{M}_y,K_t}(x, y, t) = \sum_{i=0}^{N_x}\sum_{j=0}^{M_y}\sum_{k=0}^{K_t} \bar{d}_{i,j,k} P_{T,k}(t) P_{X,i}(x) P_{Y,j}(y)$ are the best approximations of the exact solutions of $\tilde{u}(x, y, t)$ and $\tilde{v}(x, y, t)$. Assume $\check{U}_{\mathcal{N}_x,\mathcal{M}_y,K_t}(x, y, t) = \sum_{i=0}^{N_x}\sum_{j=0}^{M_y}\sum_{k=0}^{K_t} \check{c}_{i,j,k} P_{T,k}(t) P_{X,i}(x) P_{Y,j}(y)$ and $\check{U}_{\mathcal{N}_x,\mathcal{M}_y,K_t}(x, y, t) = \sum_{i=0}^{N_x}\sum_{j=0}^{M_y}\sum_{k=0}^{K_t} \check{d}_{i,j,k} P_{T,k}(t) P_{X,i}(x) P_{Y,j}(y)$ be the numerical solutions obtained by the proposed scheme. Then, we obtain*

$$||\tilde{U}_{N_x,M_y,K_t}(x, y, t) - \tilde{u}_{N_x,M_y,K_t}(x, y, t)||_{L_2} \le ||\bar{C} - \check{C}||_2 \left(\sum_{i=0}^{N_x}\sum_{j=0}^{M_y}\sum_{k=0}^{K_t} \frac{XYT}{(2i+1)(2j+1)(2k+1)}\right)^{\frac{1}{2}}, \tag{26}$$

$$||\tilde{V}_{N_x,M_y,K_t}(x,y,t)-\tilde{v}_{N_x,M_y,K_t}(x,y,t)||_{L_2}\le||\bar{D}-\breve{D}||_2\left(\sum_{i=0}^{N_x}\sum_{j=0}^{M_y}\sum_{k=0}^{K_t}\frac{XYT}{(2i+1)(2j+1)(2k+1)}\right)^{\frac{1}{2}}, \tag{27}$$

where

$$\|\bar{C}-\breve{C}\|_{L_2}=\left(\sum_{i=0}^{N_x}\sum_{j=0}^{M_y}\sum_{k=0}^{K_t}(|\bar{c}_{i,j,k}-\breve{c}_{i,j,k}|^2)\right)^{\frac{1}{2}},$$

$$\|\bar{D}-\breve{D}\|_{L_2}=\left(\sum_{i=0}^{N_x}\sum_{j=0}^{M_y}\sum_{k=0}^{K_t}(|\bar{d}_{i,j,k}-\breve{d}_{i,j,k}|^2)\right)^{\frac{1}{2}}.$$

Theorem 3 [42] *Let us consider $\tilde{u}_{N_x,M_y,K_t}(x,y,t)$ and $\tilde{v}_{N_x,M_y,K_t}(x,y,t)$ are the approximations of $\tilde{u}(x,y,t)$ and $\tilde{v}(x,y,t)$ obtained by the proposed method. Then, we obtain*

$$\begin{aligned}||\tilde{u}(x,y,t)-\tilde{u}_{N_x,M_y,K_t}(x,y,t)||_{L_2}\le(XYT)^{\frac{1}{2}}A_1&\left(\frac{1}{4}\left(\frac{X}{N_x}\right)^{N_x+1}+\frac{1}{4}\left(\frac{Y}{M_y}\right)^{M_y+1}+\frac{1}{4}\left(\frac{T}{K_t}\right)^{K_t+1}\right.\\&\left.+\frac{1}{64}\left(\frac{X}{N_x}\right)^{N_x+1}\left(\frac{Y}{M_y}\right)^{M_y+1}\left(\frac{T}{K_t}\right)^{K_t+1}\right)+||\bar{C}-\tilde{C}||_{L_2}\\&\times\left(\sum_{i=0}^{N_x}\sum_{j=0}^{M_y}\sum_{k=0}^{K_t}\frac{XYT}{(2i+1)(2j+1)(2k+1)}\right)^{\frac{1}{2}},\end{aligned} \tag{28}$$

$$\begin{aligned}||\tilde{v}(x,y,t)-\tilde{v}_{N_x,M_y,K_t}(x,y,t)||_{L_2}\le(XYT)^{\frac{1}{2}}A_2&\left(\frac{1}{4}\left(\frac{X}{N_x}\right)^{N_x+1}+\frac{1}{4}\left(\frac{Y}{M_y}\right)^{M_y+1}+\frac{1}{4}\left(\frac{T}{K_t}\right)^{K_t+1}\right.\\&\left.+\frac{1}{64}\left(\frac{X}{N_x}\right)^{N_x+1}\left(\frac{Y}{M_y}\right)^{M_y+1}\left(\frac{T}{K_t}\right)^{K_t+1}\right)+||\bar{D}-\tilde{D}||_{L_2}\\&\times\left(\sum_{i=0}^{N_x}\sum_{j=0}^{M_y}\sum_{k=0}^{K_t}\frac{XYT}{(2i+1)(2j+1)(2k+1)}\right)^{\frac{1}{2}}.\end{aligned} \tag{29}$$

Theorem 4 [42] *Let $w1_{N_x,M_y,K_t}(x,y,t)$, $w2_{N_x,M_y,K_t}(x,y,t)$, $w3_{N_x,M_y,K_t}(x,y,t)$, $w4_{N_x,M_y,K_t}(x,y,t)$, $w5_{N_x,M_y,K_t}(x,y,t)$, $w6_{N_x,M_y,K_t}(x,y,t)$, $w7_{N_x,M_y,K_t}(x,y,t)$, $w8_{N_x,M_y,K_t}(x,y,t)$, $g1_{N_x,M_y,K_t}(x,y,t)$ and $g2_{N_x,M_y,K_t}(x,y,t)$, are approximations of $w_1(x,y,t)$, $w_2(x,y,t)$, $w_3(x,y,t)$, $w_4(x,y,t)$, $w_5(x,y,t)$, $w_6(x,y,t)$, $w_7(x,y,t)$, $w_8(x,y,t)$, $g_1(x,y,t)$ and $g_2(x,y,t)$, which satisfy the assumption of Theorem 1, where $\frac{\partial\tilde{u}(x,y,t)}{\partial t}=w_1(x,y,t)$, $\frac{\partial^2\tilde{u}(x,y,t)}{\partial x^2}=w_2(x,y,t)$, $\frac{\partial^2\tilde{u}(x,y,t)}{\partial y^2}=w_3(x,y,t)$, $\frac{\partial\tilde{u}(x,y,t)}{\partial x}=w_4(x,y,t)$, $\frac{\partial\tilde{v}(x,y,t)}{\partial t}=w_5(x,y,t)$, $\frac{\partial^2\tilde{v}(x,y,t)}{\partial x^2}=w_6(x,y,t)$, $\frac{\partial^2\tilde{v}(x,y,t)}{\partial y^2}=w_7(x,y,t)$, $\frac{\partial\tilde{v}(x,y,t)}{\partial y}=w_8(x,y,t)$. Then, we have*

$$\begin{aligned}||H(x,y,t)-H_{N_x,M_y,K_t}(x,y,t)||_{L_2}\le(XYT)^{\frac{1}{2}}A_n&\left(\frac{1}{4}\left(\frac{X}{N_x}\right)^{N_x+1}+\frac{1}{4}\left(\frac{Y}{M_y}\right)^{M_y+1}+\frac{1}{4}\left(\frac{T}{K_t}\right)^{K_t+1}\right.\\&\left.+\frac{1}{64}\left(\frac{X}{N_x}\right)^{N_x+1}\left(\frac{Y}{M_y}\right)^{M_y+1}\left(\frac{T}{K_t}\right)^{K_t+1}\right),\end{aligned} \tag{30}$$

where $H\in\{w_1,w_2,w_3,w_4,w_5,w_6,w_7,w_8,g_1,g_2\}$, $\mathcal{A}_n\in\{\mathcal{A}_3,\mathcal{A}_4,\mathcal{A}_5,\mathcal{A}_6,\mathcal{A}_7,\mathcal{A}_8,\mathcal{A}_9,\mathcal{A}_{10}\ \mathcal{A}_{11},\mathcal{A}_{12}\}$ and $\mathcal{A}_n = \max\Big\{\max\left|\frac{\partial^{N_x+1}H(x,y,t)}{\partial x^{N_x+1}}\right|, \max\left|\frac{\partial^{M_y+1}H(x,y,t)}{\partial y^{M_y+1}}\right|, \max\left|\frac{\partial^{K_t+1}H(x,y,t)}{\partial t^{K_t+1}}\right|, \max$

$\left|\frac{\partial^{N_x+M_y+K_t+3}H(x,y,t)}{\partial x^{N_x+1}\partial y^{M_y+1}\partial t^{K_t+1}}\right|\Big\}$ *at* $(x,y)\in[0,X]\times[0,Y]$ *and* $t\in[0,T]$. *Here* A_{n}, $\mathrm{n}=3,4,...,12$ *are given in Appendix A.*

Theorem 5 *Let* $\tilde{u}^2{}_{N_x,M_y,K_t}(x,y,t)$, $\tilde{u}^2(x,y,t)$, *be the approximate and exact solutions, respectively, then*

$$||\tilde{u}^2(x,y,t)-\tilde{u}^2_{N_x,M_y,K_t}(x,y,t)||_{L_2}\le(XYT)^{\frac{1}{2}}A_{13}\Bigg(\frac{1}{4}\left(\frac{X}{M_x}\right)^{N_x+1}+\frac{1}{4}\left(\frac{Y}{M_y}\right)^{M_y+1}+\frac{1}{4}\left(\frac{T}{K_t}\right)^{K_t+1}+\frac{1}{64}\left(\frac{X}{N_x}\right)^{N_x+1}\left(\frac{Y}{M_y}\right)^{M_y+1}\left(\frac{T}{K_t}\right)^{K_t+1}\Bigg). \tag{31}$$

Proof We known that the product of two sufficiently smooth functions is a sufficiently smooth functions, we have

$$||\tilde{u}^2(x,y,t)-\tilde{u}^2_{N_x,M_y,K_t}(x,y,t)||_{L_2}\le(XYT)^{\frac{1}{2}}A_{13}\Bigg(\frac{1}{4}\left(\frac{X}{N_x}\right)^{N_x+1}+\frac{1}{4}\left(\frac{Y}{M_y}\right)^{M_y+1}+\frac{1}{4}\left(\frac{T}{K_t}\right)^{K_t+1}+\frac{1}{64}\left(\frac{X}{N_x}\right)^{N_x+1}\left(\frac{Y}{M_y}\right)^{M_y+1}\left(\frac{T}{K_t}\right)^{K_t+1}\Bigg), \tag{32}$$

where A_{13} is given in Appendix A.

Similarly, we can find the above calculations for $\tilde{u}\tilde{v}$ and $\tilde{v}^2$

$$||(\tilde{u}\tilde{v})(x,y,t)-(\tilde{u}\tilde{v})_{N_x,M_y,K_t}(x,y,t)||_{L_2}\le(XYT)^{\frac{1}{2}}A_{14}\Bigg(\frac{1}{4}\left(\frac{X}{N_x}\right)^{N_x+1}+\frac{1}{4}\left(\frac{Y}{M_y}\right)^{M_y+1}+\frac{1}{4}\left(\frac{T}{K_t}\right)^{K_t+1}+\frac{1}{64}\left(\frac{X}{N_x}\right)^{N_x+1}\left(\frac{Y}{M_y}\right)^{M_y+1}\left(\frac{T}{K_t}\right)^{K_t+1}\Bigg), \tag{33}$$

$$||\tilde{v}^2(x,y,t)-\tilde{v}^2_{N_x,M_y,K_t}(x,y,t)||_{L_2}\le(XYT)^{\frac{1}{2}}A_{15}\Bigg(\frac{1}{4}\left(\frac{X}{N_x}\right)^{N_x+1}+\frac{1}{4}\left(\frac{Y}{M_y}\right)^{M_y+1}+\frac{1}{4}\left(\frac{T}{K_t}\right)^{K_t+1}+\frac{1}{64}\left(\frac{X}{N_x}\right)^{N_x+1}\left(\frac{Y}{M_y}\right)^{M_y+1}\left(\frac{T}{K_t}\right)^{K_t+1}\Bigg), \tag{34}$$

where A_{14} and A_{15} are given in Appendix A. □

Theorem 6 *Let* $\left(\frac{\partial^\gamma\tilde{u}(x,y,t)}{\partial t^\gamma}\right)_{N_x,M_y,K_t}$ *be approximate solution of* $\frac{\partial^\gamma\tilde{u}(x,y,t)}{\partial t^\gamma}$, *then*

$$\left|\left|\frac{\partial^\gamma\tilde{u}(x,y,t)}{\partial t^\gamma}-\left(\frac{\partial^\gamma\tilde{u}(x,y,t)}{\partial t^\gamma}\right)_{N_x,M_y,K_t}\right|\right|_{L_2}\le\frac{T^{-\gamma+1}}{\Gamma(2-\gamma)}(XYT)^{\frac{1}{2}}A_3\Bigg(\frac{1}{4}\left(\frac{X}{N_x}\right)^{N_x+1}+\frac{1}{4}\left(\frac{Y}{M_y}\right)^{M_y+1}+\frac{1}{4}\left(\frac{T}{K_t}\right)^{K_t+1}+\frac{1}{64}\left(\frac{X}{N_x}\right)^{N_x+1}\left(\frac{Y}{M_y}\right)^{M_y+1}\left(\frac{T}{K_t}\right)^{K_t+1}\Bigg).$$

Proof Consider the term $\left|\left|\frac{\partial^\gamma\tilde{u}(x,y,t)}{\partial t^\gamma}\text{ - }\left(\frac{\partial^\gamma\tilde{u}(x,y,t)}{\partial t^\gamma}\right)_{N_x,M_y,K_t}\right|\right|_{L_2}$ and using Eqs. (4), we have

$$\begin{aligned}&\left|\left|\frac{\partial^\gamma\tilde{u}(x,y,t)}{\partial t^\gamma}-\left(\frac{\partial^\gamma\tilde{u}(x,y,t)}{\partial t^\gamma}\right)_{N_x,M_y,K_t}\right|\right|_{L_2}\\&=\left|\left|\frac{1}{\Gamma(1-\gamma)}\int_0^t(t-\tau)^{-\gamma}\left(\frac{\partial^\gamma\tilde{u}(x,y,\tau)}{\partial\tau^\gamma}-\left(\frac{\partial^\gamma\tilde{u}(x,y,\tau)}{\partial\tau^\gamma}\right)_{N_x,M_y,K_t}\right)d\tau\right|\right|_{L_2}\end{aligned}$$

Using the inequality (24) and integral property given as

$$\Big|\Big|\int_0^t f(\varkappa,\tau)g(\varkappa,\tau)d\tau\Big|\Big| \le M\int_0^t \big|\big|f(\varkappa,\tau)\big|\big|d\tau,\ where\ \big|\big|g(\varkappa,\tau)\big|\big| \le M,$$

we get

$$\begin{aligned}
&\le \left(\frac{1}{\Gamma(1-\gamma)}\int_0^t (t-\tau)^{-\gamma}d\tau\right)\left\|\frac{\partial^\gamma \tilde{u}(x,y,t)}{\partial t^\gamma}-\left(\frac{\partial^\gamma \tilde{u}(x,y,t)}{\partial t^\gamma}\right)_{N_x,M_y,K_t}\right\|_{L_2}\\
&= \left(\frac{1}{\Gamma(1-\gamma)}(t)^{-\gamma+1}\frac{1}{(1-\gamma)}\right)\left\|\frac{\partial^\gamma \tilde{u}(x,y,t)}{\partial t^\gamma}-\left(\frac{\partial^\gamma \tilde{u}(x,y,t)}{\partial t^\gamma}\right)_{N_x,M_y,K_t}\right\|_{L_2}\\
&\le \frac{T^{-\gamma+1}}{\Gamma(2-\gamma)}(XYT)^{\frac{1}{2}}A_3\left(\frac{1}{4}\left(\frac{X}{N_x}\right)^{N_x+1}+\frac{1}{4}\left(\frac{Y}{M_y}\right)^{M_y+1}+\frac{1}{4}\left(\frac{T}{K_t}\right)^{K_t+1}\right.\\
&\quad\left.+\frac{1}{64}\left(\frac{X}{N_x}\right)^{N_x+1}\left(\frac{Y}{M_y}\right)^{M_y+1}\left(\frac{T}{K_t}\right)^{K_t+1}\right). \qquad (35)
\end{aligned}$$

Similarly, we can find

$$\begin{aligned}
\left\|\frac{\partial^\gamma \tilde{v}(x,y,t)}{\partial t^\gamma}-\left(\frac{\partial^\gamma \tilde{v}(x,y,t)}{\partial t^\gamma}\right)_{N_x,M_y,K_t}\right\|_{L_2} &\le \frac{T^{-\gamma+1}}{\Gamma(2-\gamma)}(XYT)^{\frac{1}{2}}A_7\left(\frac{1}{4}\left(\frac{X}{N_x}\right)^{N_x+1}+\frac{1}{4}\left(\frac{Y}{M_y}\right)^{M_y+1}\right.\\
&\quad\left.+\frac{1}{4}\left(\frac{T}{K_t}\right)^{K_t+1}+\frac{1}{64}\left(\frac{X}{N_x}\right)^{N_x+1}\left(\frac{Y}{M_y}\right)^{M_y+1}\left(\frac{T}{K_t}\right)^{K_t+1}\right), \qquad (36)
\end{aligned}$$

$$\begin{aligned}
\left\|\frac{\partial^\alpha \tilde{u}(x,y,t)}{\partial x^\alpha}-\left(\frac{\partial^\alpha \tilde{u}(x,y,t)}{\partial x^\alpha}\right)_{N_x,M_y,K_t}\right\|_{L_2} &\le \frac{X^{-\alpha+1}}{\Gamma(2-\alpha)}(XYT)^{\frac{1}{2}}A_6\left(\frac{1}{4}\left(\frac{X}{N_x}\right)^{N_x+1}+\frac{1}{4}\left(\frac{Y}{M_y}\right)^{M_y+1}\right.\\
&\quad\left.+\frac{1}{4}\left(\frac{T}{K_t}\right)^{K_t+1}+\frac{1}{64}\left(\frac{X}{N_x}\right)^{N_x+1}\left(\frac{Y}{M_y}\right)^{M_y+1}\left(\frac{T}{K_t}\right)^{K_t+1}\right), \qquad (37)
\end{aligned}$$

$$\begin{aligned}
\left\|\frac{\partial^\beta \tilde{v}(x,y,t)}{\partial y^\beta}-\left(\frac{\partial^\beta \tilde{v}(x,y,t)}{\partial y^\beta}\right)_{N_x,M_y,K_t}\right\|_{L_2} &\le \frac{Y^{-\beta+1}}{\Gamma(2-\beta)}(XYT)^{\frac{1}{2}}A_{10}\left(\frac{1}{4}\left(\frac{X}{N_x}\right)^{N_x+1}+\frac{1}{4}\left(\frac{Y}{M_y}\right)^{M_y+1}\right.\\
&\quad\left.+\frac{1}{4}\left(\frac{T}{K_t}\right)^{K_t+1}+\frac{1}{64}\left(\frac{X}{N_x}\right)^{N_x+1}\left(\frac{Y}{M_y}\right)^{M_y+1}\left(\frac{T}{K_t}\right)^{K_t+1}\right), \qquad (38)
\end{aligned}$$

□

Now, using Eqs. (30)–(38) and large values of N_x, M_y, K_t, the approximate solution convergence to exact solution. Substituting Eqs. (30)–(38), in Eqs. (5) and (6), the error bounds have been studied for the following cases when $\alpha,\beta,\gamma\in(0,1)$; $\alpha=1,\ \beta,\gamma\in(0,1)$; $\beta=1,\ \alpha,\gamma\in(0,1)$; and $\gamma=1,\ \alpha,\beta\in(0,1)$.

Case 1 When $\alpha,\beta,\gamma\in(0,1)$,

$$\begin{aligned}
&\Bigg|\Bigg|\left(\frac{\partial^\gamma \tilde{u}(x,y,t)}{\partial t^\gamma}-\left(\frac{\partial^\gamma \tilde{u}(x,y,t)}{\partial t^\gamma}\right)_{N_x,M_y,K_t}\right)-\left(\frac{\partial^{1+\alpha}\tilde{u}(x,y,t)}{\partial x^{1+\alpha}}-\left(\frac{\partial^{1+\alpha}\tilde{u}(x,y,t)}{\partial x^{1+\alpha}}\right)_{N_x,M_y,K_t}\right)\\
&-\left(\frac{\partial^{1+\beta}\tilde{u}(x,y,t)}{\partial y^{1+\beta}}-\left(\frac{\partial^{1+\beta}\tilde{u}(x,y,t)}{\partial y^{1+\beta}}\right)_{N_x,M_y,K_t}\right)-\nu_1\left(\frac{\partial^\alpha \tilde{u}(x,y,t)}{\partial x^\alpha}-\left(\frac{\partial^\alpha \tilde{u}(x,y,t)}{\partial x^\alpha}\right)_{N_x,M_y,K_t}\right)\\
&-\lambda_1\left(\tilde{u}^2(x,y,t)-\tilde{u}^2_{N_x,M_y,K_t}(x,y,t)\right)+\lambda_1\left(\tilde{u}(x,y,t)\times\tilde{v}(x,y,t)-\left(\tilde{u}(x,y,t)\times\tilde{v}(x,y,t)\right)_{N_x,M_y,K_t}\right)
\end{aligned}$$

$$
\begin{aligned}
&-\left(g_1(x,y,t)-g_{1_{N_x,M_y,K_t}}(x,y,t)\right)\Bigg\|_{L_2}\\
&\leq \frac{T^{-\gamma+1}}{\Gamma(2-\gamma)}(XYT)^{\frac{1}{2}}\mathcal{A}_3\left(\frac{1}{4}\left(\frac{X}{N_x}\right)^{N_x+1}+\frac{1}{4}\left(\frac{Y}{M_y}\right)^{M_y+1}+\frac{1}{4}\left(\frac{T}{K_t}\right)^{K_t+1}+\frac{1}{64}\left(\frac{X}{N_x}\right)^{N_x+1}\left(\frac{Y}{M_y}\right)^{M_y+1}\right.\\
&\left.\times\left(\frac{T}{K_t}\right)^{K_t+1}\right)-\frac{X^{-\alpha+1}}{\Gamma(2-\alpha)}(XYT)^{\frac{1}{2}}\mathcal{A}_4\left(\frac{1}{4}\left(\frac{X}{N_x}\right)^{N_x+1}+\frac{1}{4}\left(\frac{Y}{M_y}\right)^{M_y+1}+\frac{1}{4}\left(\frac{T}{K_t}\right)^{K_t+1}+\frac{1}{64}\left(\frac{X}{N_x}\right)^{N_x+1}\right.\\
&\left.\times\left(\frac{Y}{M_y}\right)^{M_y+1}\left(\frac{T}{K_t}\right)^{K_t+1}\right)-\frac{Y^{-\beta+1}}{\Gamma(2-\beta)}(XYT)^{\frac{1}{2}}\mathcal{A}_5\left(\frac{1}{4}\left(\frac{X}{N_x}\right)^{N_x+1}+\frac{1}{4}\left(\frac{Y}{M_y}\right)^{M_y+1}+\frac{1}{4}\left(\frac{T}{K_t}\right)^{K_t+1}\right.\\
&\left.+\frac{1}{64}\left(\frac{X}{N_x}\right)^{N_x+1}\left(\frac{Y}{M_y}\right)^{M_y+1}\left(\frac{T}{K_t}\right)^{K_t+1}\right)-\nu_1\frac{X^{-\alpha+1}}{\Gamma(2-\alpha)}(XYT)^{\frac{1}{2}}\mathcal{A}_6\left(\frac{1}{4}\left(\frac{X}{N_x}\right)^{N_x+1}+\frac{1}{4}\left(\frac{Y}{M_y}\right)^{M_y+1}\right.\\
&\left.+\frac{1}{4}\left(\frac{T}{K_t}\right)^{K_t+1}+\frac{1}{64}\left(\frac{X}{N_x}\right)^{N_x+1}\left(\frac{Y}{M_y}\right)^{M_y+1}\left(\frac{T}{K_t}\right)^{K_t+1}\right)-\lambda_1(XYT)^{\frac{1}{2}}\mathcal{A}_{13}\left(\frac{1}{4}\left(\frac{X}{N_x}\right)^{N_x+1}+\frac{1}{4}\left(\frac{Y}{M_y}\right)^{M_y+1}\right.\\
&\left.+\frac{1}{4}\left(\frac{T}{K_t}\right)^{K_t+1}+\frac{1}{64}\left(\frac{X}{N_x}\right)^{N_x+1}\left(\frac{Y}{M_y}\right)^{M_y+1}\left(\frac{T}{K_t}\right)^{K_t+1}\right)+\lambda_1(XYT)^{\frac{1}{2}}\mathcal{A}_{14}\left(\frac{1}{4}\left(\frac{X}{N_x}\right)^{N_x+1}+\frac{1}{4}\left(\frac{Y}{M_y}\right)^{M_y+1}\right.\\
&\left.+\frac{1}{4}\left(\frac{T}{K_t}\right)^{K_t+1}+\frac{1}{64}\left(\frac{X}{N_x}\right)^{N_x+1}\left(\frac{Y}{M_y}\right)^{M_y+1}\left(\frac{T}{K_t}\right)^{K_t+1}\right)-(XYT)^{\frac{1}{2}}\mathcal{A}_{11}\left(\frac{1}{4}\left(\frac{X}{N_x}\right)^{N_x+1}+\frac{1}{4}\left(\frac{Y}{M_y}\right)^{M_y+1}\right.\\
&\left.+\frac{1}{4}\left(\frac{T}{K_t}\right)^{K_t+1}+\frac{1}{64}\left(\frac{X}{N_x}\right)^{N_x+1}\left(\frac{Y}{M_y}\right)^{M_y+1}\left(\frac{T}{K_t}\right)^{K_t+1}\right).
\end{aligned}
\tag{39}
$$

Similarly,

$$
\begin{aligned}
&\Bigg\|\left(\frac{\partial^{\gamma}\tilde{v}(x,y,t)}{\partial t^{\gamma}}-\left(\frac{\partial^{\gamma}\tilde{v}(x,y,t)}{\partial t^{\gamma}}\right)_{N_x,M_y,K_t}\right)-\left(\frac{\partial^{1+\alpha}\tilde{v}(x,y,t)}{\partial x^{1+\alpha}}-\left(\frac{\partial^{1+\alpha}\tilde{v}(x,y,t)}{\partial x^{1+\alpha}}\right)_{N_x,M_y,K_t}\right)\\
&-\left(\frac{\partial^{1+\beta}\tilde{v}(x,y,t)}{\partial y^{1+\beta}}-\left(\frac{\partial^{1+\beta}\tilde{v}(x,y,t)}{\partial y^{1+\beta}}\right)_{N_x,M_y,K_t}\right)-\nu_2\left(\frac{\partial^{\beta}\tilde{v}(x,y,t)}{\partial x^{\beta}}-\left(\frac{\partial^{\beta}\tilde{v}(x,y,t)}{\partial x^{\beta}}\right)_{N_x,M_y,K_t}\right)\\
&-\lambda_2\left(\tilde{v}^2(x,y,t)-\tilde{v}^2_{N_x,M_y,K_t}(x,y,t)\right)+\lambda_2\left(\tilde{v}(x,y,t)\times\tilde{u}(x,y,t)-\left(\tilde{v}(x,y,t)\times\tilde{u}(x,y,t)\right)_{N_x,M_y,K_t}\right)\\
&-\left(g_2(x,y,t)-g_{2_{N_x,M_y,K_t}}(x,y,t)\right)\Bigg\|_{L_2}\\
&\leq \frac{T^{-\gamma+1}}{\Gamma(2-\gamma)}(XYT)^{\frac{1}{2}}\mathcal{A}_7\left(\frac{1}{4}\left(\frac{X}{N_x}\right)^{N_x+1}+\frac{1}{4}\left(\frac{Y}{M_y}\right)^{M_y+1}+\frac{1}{4}\left(\frac{T}{K_t}\right)^{K_t+1}+\frac{1}{64}\left(\frac{X}{N_x}\right)^{N_x+1}\left(\frac{Y}{M_y}\right)^{M_y+1}\right.\\
&\left.\times\left(\frac{T}{K_t}\right)^{K_t+1}\right)-\frac{X^{-\alpha+1}}{\Gamma(2-\alpha)}(XYT)^{\frac{1}{2}}\mathcal{A}_8\left(\frac{1}{4}\left(\frac{X}{N_x}\right)^{N_x+1}+\frac{1}{4}\left(\frac{Y}{M_y}\right)^{M_y+1}+\frac{1}{4}\left(\frac{T}{K_t}\right)^{K_t+1}+\frac{1}{64}\left(\frac{X}{N_x}\right)^{N_x+1}\right.\\
&\left.\times\left(\frac{Y}{M_y}\right)^{M_y+1}\left(\frac{T}{K_t}\right)^{K_t+1}\right)-\frac{Y^{-\beta+1}}{\Gamma(2-\beta)}(XYT)^{\frac{1}{2}}\mathcal{A}_9\left(\frac{1}{4}\left(\frac{X}{N_x}\right)^{N_x+1}+\frac{1}{4}\left(\frac{Y}{M_y}\right)^{M_y+1}+\frac{1}{4}\left(\frac{T}{K_t}\right)^{K_t+1}\right.\\
&\left.+\frac{1}{64}\left(\frac{X}{N_x}\right)^{N_x+1}\left(\frac{Y}{M_y}\right)^{M_y+1}\left(\frac{T}{K_t}\right)^{K_t+1}\right)-\nu_1\frac{X^{-\alpha+1}}{\Gamma(2-\alpha)}(XYT)^{\frac{1}{2}}\mathcal{A}_{10}\left(\frac{1}{4}\left(\frac{X}{N_x}\right)^{N_x+1}+\frac{1}{4}\left(\frac{Y}{M_y}\right)^{M_y+1}\right.\\
&\left.+\frac{1}{4}\left(\frac{T}{K_t}\right)^{K_t+1}+\frac{1}{64}\left(\frac{X}{N_x}\right)^{N_x+1}\left(\frac{Y}{M_y}\right)^{M_y+1}\left(\frac{T}{K_t}\right)^{K_t+1}\right)-\lambda_1(XYT)^{\frac{1}{2}}\mathcal{A}_{15}\left(\frac{1}{4}\left(\frac{X}{N_x}\right)^{N_x+1}+\frac{1}{4}\left(\frac{Y}{M_y}\right)^{M_y+1}\right.\\
&\left.+\frac{1}{4}\left(\frac{T}{K_t}\right)^{K_t+1}+\frac{1}{64}\left(\frac{X}{N_x}\right)^{N_x+1}\left(\frac{Y}{M_y}\right)^{M_y+1}\left(\frac{T}{K_t}\right)^{K_t+1}\right)+\lambda_1(XYT)^{\frac{1}{2}}\mathcal{A}_{14}\left(\frac{1}{4}\left(\frac{X}{N_x}\right)^{N_x+1}+\frac{1}{4}\left(\frac{Y}{M_y}\right)^{M_y+1}\right.\\
&\left.+\frac{1}{4}\left(\frac{T}{K_t}\right)^{K_t+1}+\frac{1}{64}\left(\frac{X}{N_x}\right)^{N_x+1}\left(\frac{Y}{M_y}\right)^{M_y+1}\left(\frac{T}{K_t}\right)^{K_t+1}\right)-(XYT)^{\frac{1}{2}}\mathcal{A}_{12}\left(\frac{1}{4}\left(\frac{X}{N_x}\right)^{N_x+1}+\frac{1}{4}\left(\frac{Y}{M_y}\right)^{M_y+1}\right.\\
&\left.+\frac{1}{4}\left(\frac{T}{K_t}\right)^{K_t+1}+\frac{1}{64}\left(\frac{X}{N_x}\right)^{N_x+1}\left(\frac{Y}{M_y}\right)^{M_y+1}\left(\frac{T}{K_t}\right)^{K_t+1}\right).
\end{aligned}
\tag{40}
$$

Table 1 MAE in the approximate solutions $\tilde{u}$ and $\tilde{v}$ at $t = 1$ with $\alpha = 0.9, \beta = 0.7, \gamma = 0.6$ for Example 1

	$\alpha = 0.9, \beta = 0.7, \gamma = 0.6$			
(N_x, M_y, K_t)	$MAE_{\tilde{u}}$	$MAE_{\tilde{v}}$	$CO.\tilde{u}$	$CO.\tilde{v}$
(3,3,3)	1.6977×10^{-4}	2.15385×10^{-4}	2.24734	3.34581
(4,4,4)	2.44074×10^{-5}	1.19992×10^{-5}	10.4272	6.07269
(5,4,4)	2.38245×10^{-6}	3.09491×10^{-6}	6.27438	11.0697
(6,4,4)	7.58945×10^{-7}	4.11279×10^{-7}	21.8145	15.6798
(7,4,4)	2.62904×10^{-8}	3.66798×10^{-8}	–	–

Thus for large values of $N_x, M_y, K_t,$ the error converges to zero. In the similar way, we can show the convergence of the said equations for other three cases for the large values of N_x, M_y, K_t.

5 Numerical analysis

In this section, the results for two test problems are presented to assess the practical performance of the proposed method. Assume that the SLGL interpolation nodes $\tilde{u}_{\mathbf{E}}(x, y, t)$ and $\tilde{u}_{N_x,M_y}(x, y, t)$ are the exact and numerical solutions, respectively. Then the Maximum Absolute Error (MAE) at $t = T$ is determined as

$$MAE_{\tilde{u}} = \max_{1\le i\le N_x, 1\le j\le M_y} \left\{ \left| \tilde{u}_{\mathbf{E}}(x_i, y_j, T) - \tilde{u}_{N_x,M_y}(x_i, y_j, T) \right| \right\}.$$

The following formula is used to evaluate the order of convergence [45] as

$$\mathrm{CO} = \frac{\log\left(\max \mathbf{E}_{\mathrm{abs}}(N_1)/ \max \mathbf{E}_{\mathrm{abs}}(N_2)\right)}{\log(N_2/N_1)}.$$

Example 1 First, let us consider the Eqs. (1) and (2) for the space-time fractional reaction-advection–diffusion in two dimensions for $(x, y) \in [0, 1] \times [0, 1]$, $t \in [0, 1]$ and with the force terms as

$$\begin{aligned} g_1(x, y, t) = {} & \frac{t\, x^{2-\alpha}\, y}{(1 - 5\alpha + (1+\alpha)^2)\Gamma(1-\alpha)} F\left[1, \left(2 - \frac{1+\alpha}{2}, \frac{5}{2} - \frac{1+\alpha}{2}\right); \frac{-x^2}{4}\right] + \frac{t\, x^{1-\alpha}\, y\, \nu_1}{(1-\alpha)\Gamma(1-\alpha)} \\ & \times F[1, (1 - \frac{\alpha}{2}, \frac{3}{2} - \frac{\alpha}{2}); \frac{-x^2}{4}] + t^3\, y^2\, \lambda_1 \cos(x) \sin(x) + \frac{t^{1-\gamma}\, y \sin(x)}{(1-\gamma)\Gamma(1-\gamma)} - t^2\, y^2 \\ & \times \lambda_1 \sin^2(x), \end{aligned}$$

$$\begin{aligned} g_2(x, y, t) = {} & - t^4\, y^2\, \lambda_2 \cos^2(x) + \frac{t^2\, y^{1-\beta}\, \nu_2 \cos(x)}{(1-\beta)\Gamma(1-\beta)} + \frac{2t^{2-\gamma}\, y \cos(x)}{(2 - 3\gamma + \gamma^2)\Gamma(1-\gamma)} + \frac{t^2\, x^{1-\alpha}\, y}{(1-\alpha)\Gamma(1-\alpha)} \\ & \times F\left[1, \left(\frac{3}{2} - \frac{1+\alpha}{2}, 2 - \frac{1+\alpha}{2}\right); \frac{-x^2}{4}\right] + t^3\, y^2\, \lambda_2 \cos(x) \sin(x). \end{aligned}$$

whose exact solutions are $\tilde{u}(x, y, t) = y\, t\, \sin(x)$, $\tilde{v}(x, y, t) = y\, t^2 \cos(x)$, which can be used to obtain the initial and boundary conditions.

In this example, using our proposed technique presented in Sect. 3, we find the approximate solutions, for $(x, y) \in [0, 1] \times [0, 1]$ and $t \in [0, 1]$, $(\alpha, \beta, \gamma) = (0.9, 0.7, 0.6)$ with the advection coefficients as $\nu_1 = 0.6$, $\nu_2 = 0.6$ and reaction coefficients as $\lambda_1 = -1$, $\lambda_2 = -1$. The graphical comparisons of the numerical solutions and their exact solutions of $\tilde{u}$ and $\tilde{v}$ with $(\alpha, \beta, \gamma) = (0.9, 0.7, 0.6)$, $(N_x, M_y, K_t) = (7, 4, 4)$ at $t = 1$ are shown in Figs. 1 and 2, where the exact and the numerical solutions are quite similar with a Maximum Absolute Error.

Tables 1 and 2 give the Max absolute errors of $\tilde{u}(x, y, t)$ and $\tilde{v}(x, y, t)$ for two different set of values of fractional derivatives $(\alpha, \beta, \gamma) = (0.9, 0.7, 0.6)$ and $(\alpha, \beta, \gamma) = (0.8, 0.7, 0.4)$.

It is clearly seen from the tabular presentations that the numerical error decreases as N_x, M_y, K_t increases, showing that the present scheme converges well. Figure 3 illustrates the behaviour of the absolute errors of $\tilde{u}$ and $\tilde{v}$ for the various values of x and y at t=1.

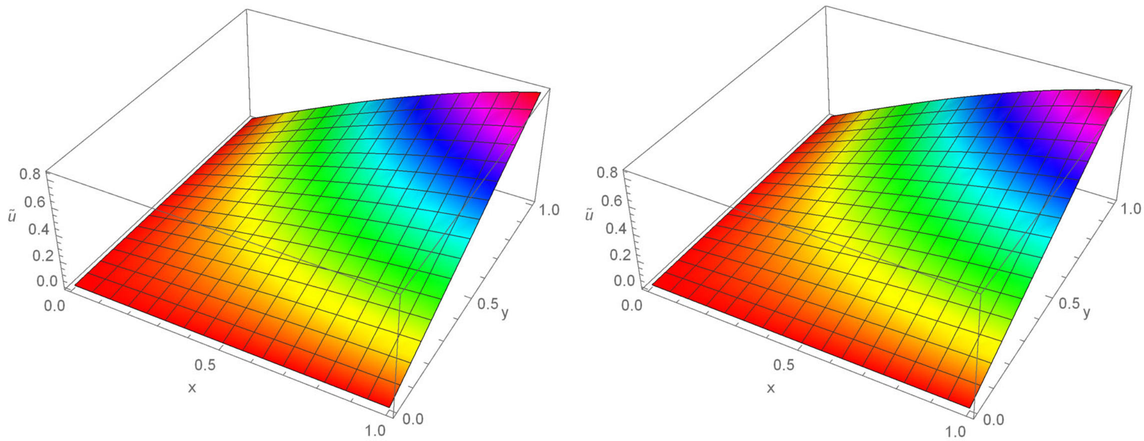

(a) (b)

Fig. 1 Plots of **a** exact solution and **b**) numerical solution of $\tilde{u}(x, y, t)$ at $t = 1$ for Example 1

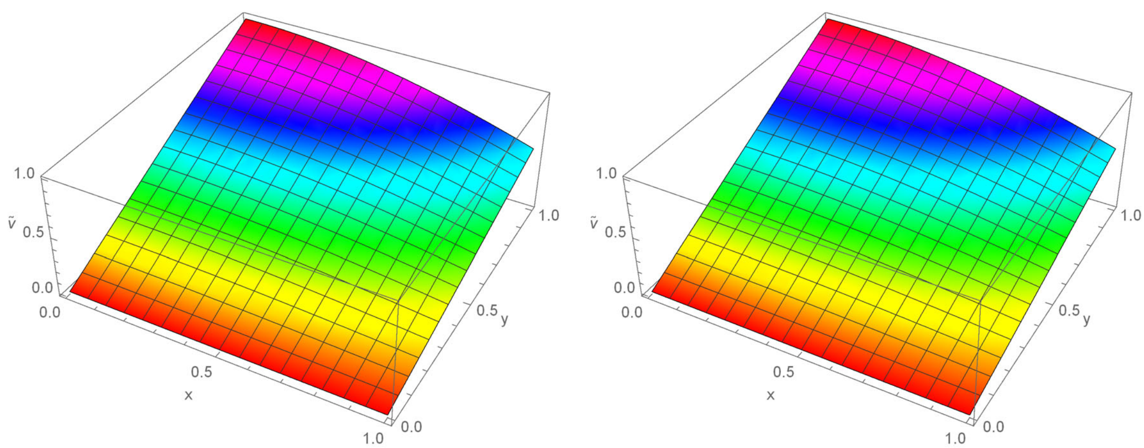

(a) (b)

Fig. 2 Plots of **a** exact solution and **b** numerical solution of $\tilde{v}(x, y, t)$ at $t = 1$ for Example 1

Table 2 MAE in the approximate solutions $\tilde{u}$ and $\tilde{v}$ at $t = 1$ with $\alpha = 0.8, \beta = 0.7, \gamma = 0.4$ for Example 1

	$\alpha = 0.8, \beta = 0.7, \gamma = 0.4$			
(N_x, M_y, K_t)	$MAE_{\tilde{u}}$	$MAE_{\tilde{v}}$	$CO.\tilde{u}$	$CO.\tilde{v}$
(3,3,3)	1.84367×10^{-4}	2.06424×10^{-4}	2.14702	3.08874
(4,4,4)	2.89031×10^{-5}	1.43566×10^{-5}	10.9146	6.66894
(5,4,4)	2.53053×10^{-6}	3.24164×10^{-6}	5.94443	10.7282
(6,4,4)	8.56099×10^{-7}	4.5845×10^{-7}	21.9859	15.8309
(7,4,4)	2.88827×10^{-8}	3.99452×10^{-8}	–	–

Example 2 Let us consider the Eqs. (1) and (2) with $(x, y) \in [0, 1] \times [0, 1]$, $t \in [0, 1]$ having force terms as

$$g_1(x, y, t) = e^{-x}\, t\, (-x)^{1+\alpha}\, x^{-\alpha}\, y + e^{-x}\, t\, (-x)^{1+\alpha}\, x^{-1-\alpha}\, y\, (1+\alpha) + e^{-x}\, t\, (-x)^{\alpha}\, x^{1-\alpha}\, y$$
$$\times\, \nu_1 - e^{-x}\, t\, (-x)^{\alpha}\, x^{-\alpha}\, y\, \alpha\, \nu_1 - \lambda_1\, e^{-2x}\, t^2\, x^2 + \frac{t\, x^{(1-\alpha)} y (1+\lambda_1)}{\Gamma(1-\alpha)}$$
$$+ \frac{1}{\Gamma(1-\alpha)}\, e^{-x}\, t\, x^{2-\alpha}\, y\, \nu_1\, E[\alpha, -x] - \frac{1}{\Gamma(1-\alpha)}\, e^{-x}\, t\, x^{1-\alpha}\, x^{-\alpha} y\, \alpha\, \nu_1\, E[\alpha, -x]$$

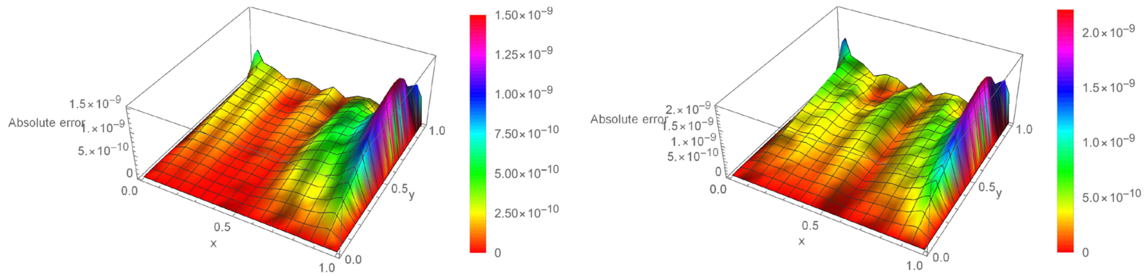

(a) (b)

Fig. 3 Plots **a** and **b** represents error graph $\tilde{u}(x, y, t)$ and $\tilde{v}(x, y, t)$ at $t = 1$ for Example 1

Table 3 MAE in the approximate solutions $\tilde{u}$ and $\tilde{v}$ at $t = 1$ with $\alpha = 0.9, \beta = 0.8, \gamma = 0.7$ for Example 2

	$\alpha = 0.9, \beta = 0.8, \gamma = 0.7$			
(N_x, M_y, K_t)	$MAE_{\tilde{u}}$	$MAE_{\tilde{v}}$	$CO.\tilde{u}$	$CO.\tilde{v}$
(3,3,3)	4.57811×10^{-4}	1.39938×10^{-4}	2.11934	2.32918
(4,4,4)	7.3506×10^{-5}	1.87465×10^{-5}	8.04149	9.76675
(5,4,4)	1.22186×10^{-5}	2.12043×10^{-6}	7.2857	6.99568
(6,4,4)	3.23691×10^{-6}	5.92239×10^{-7}	18.2326	21.9403
(7,4,4)	1.94767×10^{-7}	2.01218×10^{-8}	–	–

Table 4 MAE in the approximate solutions $\tilde{u}$ and $\tilde{v}$ at $t = 1$ with $\alpha = 0.8, \beta = 0.7, \gamma = 0.4$ for Example 2

	$\alpha = 0.8, \beta = 0.7, \gamma = 0.4$			
(N_x, M_y, K_t)	$MAE_{\tilde{u}}$	$MAE_{\tilde{v}}$	$CO.\tilde{u}$	$CO.\tilde{v}$
(3,3,3)	5.19718×10^{-4}	1.48218×10^{-4}	1.9992	2.0048
(4,4,4)	9.25629×10^{-5}	2.62706×10^{-5}	8.60461	10.6934
(5,4,4)	1.35695×10^{-5}	2.41644×10^{-6}	6.80543	6.66507
(6,4,4)	3.92375×10^{-6}	7.16849×10^{-7}	18.5661	22.5584
(7,4,4)	2.24265×10^{-7}	2.2142×10^{-8}	–	–

$$
\begin{aligned}
&+ \frac{1}{(1-\gamma)\Gamma(1-\gamma)}\, e^{-x}\, t^{1-\gamma}\, x\, y + \frac{1}{\Gamma(1-\alpha)} e^{-x}\, t\, (-x)^{1+\alpha} x^{-\alpha}\, y \Gamma(1-\alpha, -x) \\
&+ \frac{1}{\Gamma(1-\alpha)}\, e^{-x}\, t\, (-x)^{1+\alpha}\, x^{1+\alpha}\, y\, \Gamma(1-\alpha, -x) + e^{-x}\, t^3\, x\, y^2\, \lambda_1 \sin(x),
\end{aligned}
$$

$$
\begin{aligned}
g_2(x, y, t) = &\frac{t^2\, y\, x^{2-\alpha}}{(1-\alpha+(1+\alpha)^2)\Gamma(1-\alpha)} F\left[1, \left(2 - \frac{1+\alpha}{2}, \frac{5}{2} - \frac{\alpha}{2}\right); \frac{-x^2}{4}\right] + e^{-x}\, t^3\, x\, y^2\, \lambda_2 \sin(x) \\
&+ \frac{t^2\, y^{1-\beta}\, \nu_2 \sin(x)}{(1-\beta)\Gamma(1-\beta)} + \frac{2t^{2-\gamma}\, y \sin(x)}{(1-\beta)\Gamma(1-\beta)} + \frac{2t^{2-\gamma}\, y \sin(x)}{(2-3\gamma+\gamma^2)\Gamma(1-\gamma)} - t^4\, y^2\, \lambda_2 \sin^2(x).
\end{aligned}
$$

whose exact solutions $\tilde{u}(x, y, t) = t\, x\, y\, e^{-x}$, $\tilde{v}(x, y, t) = t^2\, y\, \sin(x)$ can be used to obtain the initial and boundary conditions.

This example is solved for a number of values of (N_x, M_y, K_t) at $t = 1$ for two different values of $(\alpha, \beta, \gamma) = (0.9, 0.8, 0.7)$ and $(\alpha, \beta, \gamma) = (0.8, 0.7, 0.4)$ with advection coefficients $\nu_1 = 0.6$, $\nu_2 = 0.6$ and reaction coefficients $\lambda_1 = -1$, $\lambda_2 = -1$. The $MAE_{\tilde{u}}$ and $MAE_{\tilde{v}}$ of the present scheme are shown in Tables 3 and 4 for the aforementioned two sets of values of (α, β, γ).

It is seen from tables that the errors converge well as the values of N_x, M_y, K_t are increased. The plots of exact and numerical values of $\tilde{u}$ and $\tilde{v}$ are shown through Figs. 4 and 5, respectively for the aforementioned values of parameters.

The absolute errors of $\tilde{u}(x, y, t)$ and $\tilde{v}(x, y, t)$ for the fractional order derivatives $(\alpha, \beta, \gamma) = (0.9, 0.8, 0.7)$ and (N_x, M_y, K_t)=(7,4,4) at t=1 are shown through Fig. 6.

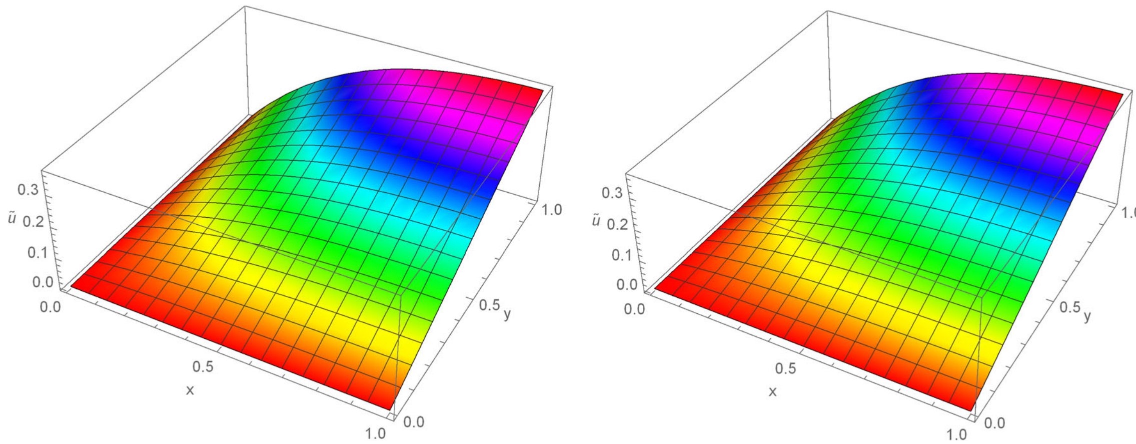

(a) (b)

Fig. 4 Plots of **a** exact solution and **b** numerical solution of $\tilde{u}(x, y, t)$ at $t = 1$ for Example 2

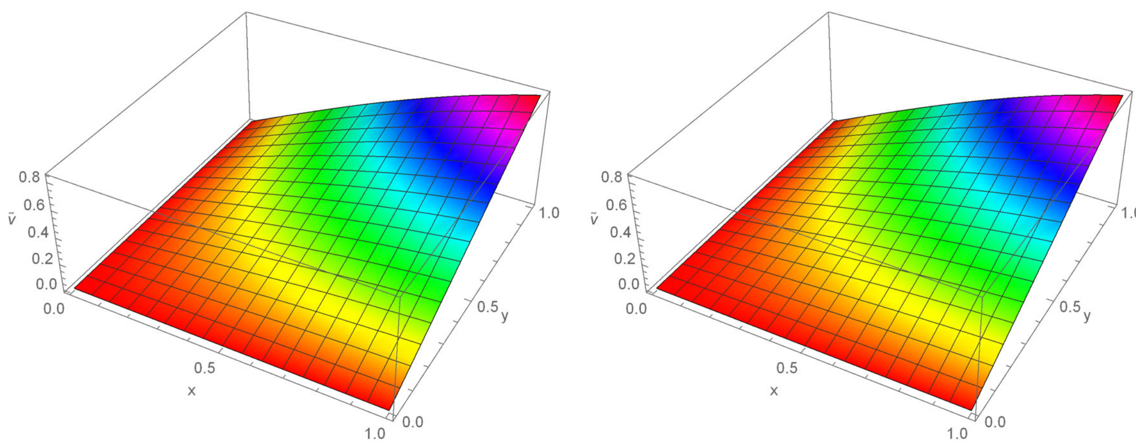

(a) (b)

Fig. 5 Plots of **a** exact solution and **b** numerical solution of $\tilde{v}(x, y, t)$ at $t = 1$ for Example 2

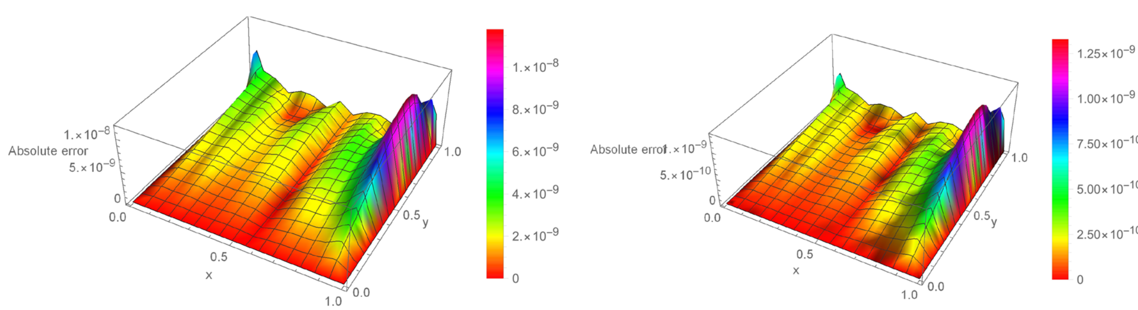

(a) (b)

Fig. 6 Plots **a** and **b** represent error graphs $\tilde{u}(x, y, t)$ and $\tilde{v}(x, y, t)$ at $t = 1$ for Example 2

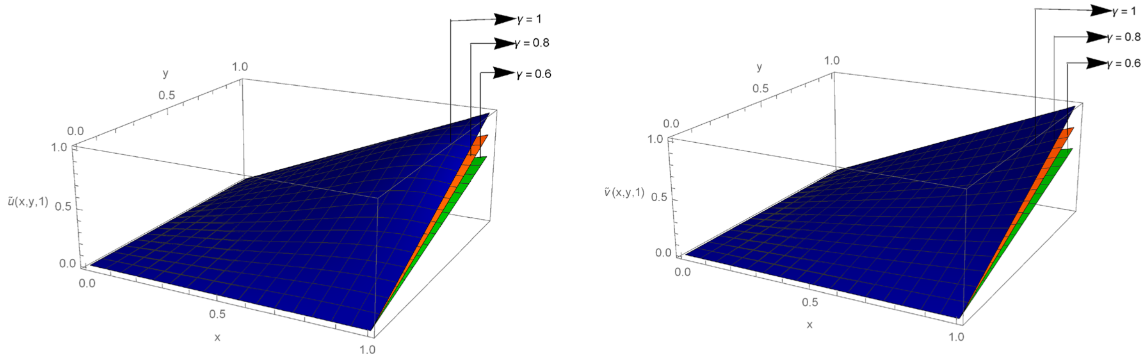

(a) (b)

Fig. 7 Plots of the concentrations of solute $\tilde{u}(x, y, t)$ and $\tilde{v}(x, y, t)$ at $t = 1$ for different values of $\gamma = 0.6, 0.8, 1$ and fixed $\alpha = 0.9,\ \beta = 0.7,\ \lambda_1 = -1,\ \nu_1 = \nu_2 = 0.6$. where $N_x, M_y, K_t = 4$

6 Application of shifted Legendre-Gauss-Lobatto collocation numerical method to solve consider 2D-STFRAD nonlinear coupled equations

After the validation of the developed algorithm given in previous section, a drive has been made to solve the mathematical model of 2D-STFRAD described the form of the in nonlinear Eqs. (1) and (2) along with the following initial and boundary conditions by using the efficient numerical scheme SLGLC for different particular cases when $(x, y) \in [0, 1] \times [0, 1],\ t \in [0, 1]$.

$$\left.\begin{array}{l}
\tilde{u}(x, y, 0) = 0 \\
\tilde{u}(0, y, t) = 0 \\
\tilde{u}(1, y, t) = (\nu_1 + 1)\ (\lambda_1 + 2)\ \alpha\ \beta\ \gamma\ y\ t \\
\tilde{u}(x, 0, t) = 0 \\
\tilde{u}(x, 1, t) = (\nu_1 + 1)\ (\lambda_1 + 2)\ \alpha\ \beta\ \gamma\ x\ t \\
\tilde{v}(x, y, 0) = 0 \\
\tilde{v}(0, y, t) = 0 \\
\tilde{v}(1, y, t) = (\nu_2 + 1)\ (\lambda_2 + 2)\ \alpha\ \beta\ \gamma\ y\ t^2 \\
\tilde{v}(x, 0, t) = 0 \\
\tilde{v}(x, 1, t) = (\nu_2 + 1)\ (\lambda_2 + 2)\ \alpha\ \beta\ \gamma\ x\ t^2
\end{array}\right\} \tag{41}$$

Here the numerical results found are depicted through graphical plots for different particular cases. Figure 7 depicts the nature of the solution profiles for different values of time fractional derivative $\gamma = 0.6, 0.8, 1$ for fixed values of $\alpha = 0.9, \beta = 0.7,$ and for advection coefficients $\nu_1 = 0.6, \nu_2 = 0.6$ and reaction coefficients $\lambda_1 = -1, \lambda_2 = -1$.

It is seen that the solute concentrations increase as γ approaches from fractional-order derivative to integer order. Figure 8 depicts the nature of the solution profile for various values of $\gamma = 0.6, 0.8, 1$ at fixed $\alpha = 0.9$, $\beta = 0.7$ for $\lambda_1 = -1, \lambda_2 = -1, \nu_1 = 0, \nu_2 = 0$.

The nature of solution profile of Fig. 8 is just the same as the Fig. 7 but due to the absence of advection terms the concentration of solute is less in each case. Fig. 9 shows the nature of the solution profile for different values of spatial derivative $\alpha = 0.2, 0.6, 1$ for the fixed values of $\beta = 0.7, \gamma = 0.6$ and advection coefficients $\nu_1 = 0.6, \nu_2 = 0.6$ and reaction coefficients as $\lambda_1 = -1, \lambda_2 = -1$.

It is seen that the solute concentration increases as fractional order derivative α approaches to integer order. Figure 10 depicts the nature of the solution profile for various values of $\alpha = 0.2, 0.6, 1$ at fixed $\beta = 0.7$, $\gamma = 0.6$ for $\lambda_1 = -1, \lambda_2 = -1, \nu_1 = 0, \nu_2 = 0$.

The nature of solution profile of Fig. 10 is just the same as the Fig. 9 but due to the absence of advection terms the concentration of solute is less in each case. Fig. 11 shows the nature of the solution profile for various values of $\beta = 0.4, 0.7, 1$ at $\alpha = 0.9, \gamma = 0.6$ at $\nu_1 = 0.6, \nu_2 = 0.6, \lambda_1 = -1, \lambda_2 = -1$.

It is seen that the solute concentration increases as β approaches to integer order derivative. Figure 12 depicts the variations of solute concentration with the variations of $\beta = 0.4, 0.7, 1$ and for fixed $\alpha = 0.9$, $\gamma = 0.6$ for $\lambda_1 = \lambda_2 = -1$, and $\nu_1 = 0, \nu_2 = 0$.

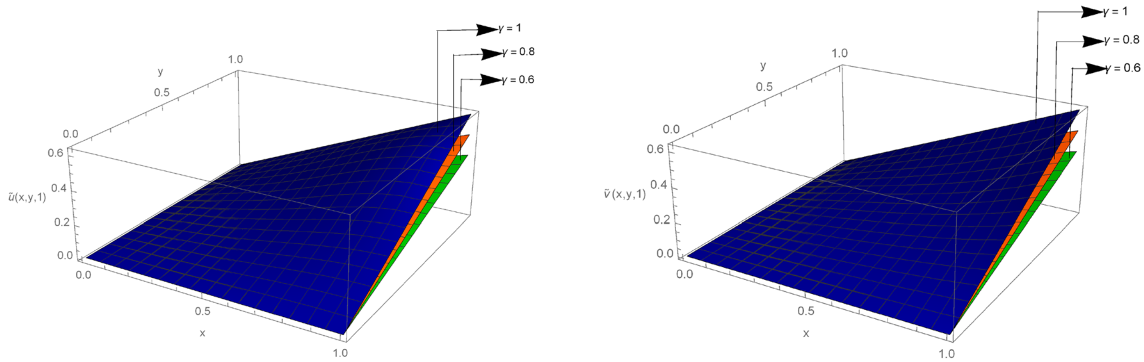

(a) (b)

Fig. 8 Plots of the concentrations of solute $\tilde{u}(x, y, t)$ and $\tilde{v}(x, y, t)$ at $t = 1$ for different values of $\gamma = 0.6, 0.8, 1$ and fixed $\alpha = 0.9$, $\beta = 0.7$, $\lambda_1 = -1$, with advection coefficients $\nu_1 = \nu_2 = 0$ where $N_x, M_y, K_t = 4$

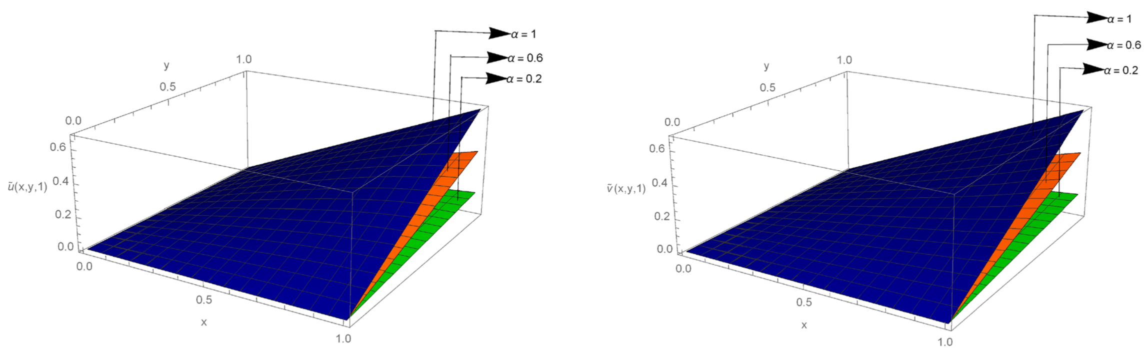

(a) (b)

Fig. 9 Plots of the concentrations of solute $\tilde{u}(x, y, t)$ and $\tilde{v}(x, y, t)$ at $t = 1$ for different values of $\alpha = 0.2, 0.6, 1$ and fixed $\beta = 0.7$, $\gamma = 0.6$, $\lambda_1 = \lambda_2 = -1$, $\nu_1 = \nu_2 = 0.6$ where $N_x, M_y, K_t = 4$

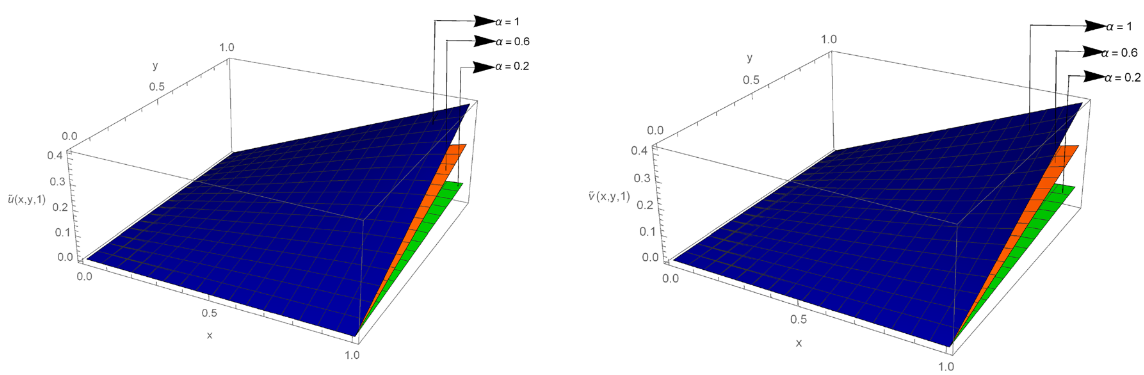

(a) (b)

Fig. 10 Plots of the concentrations of solute $\tilde{u}(x, y, t)$ and $\tilde{v}(x, y, t)$ at $t = 1$ for different values of $\alpha = 0.2, 0.6, 1$ and fixed $\beta = 0.7$, $\gamma = 0.6$, $\lambda_1 = \lambda_2 = -1$, with advection coefficients $\nu_1 = \nu_2 = 0$ where $N_x, M_y, K_t = 4$

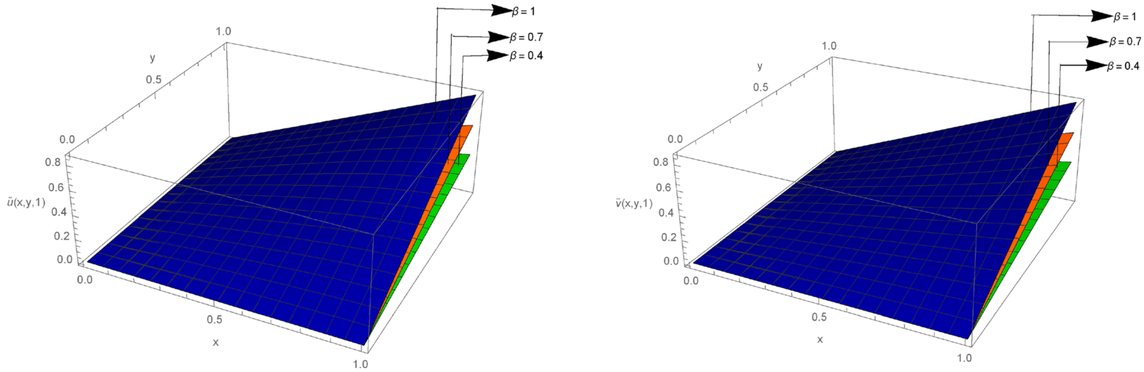

(a) (b)

Fig. 11 Plots of the concentrations of solute $\tilde{u}(x, y, t)$ and $\tilde{v}(x, y, t)$ at $t = 1$ for different values of $\beta = 0.4, 0.7, 1$ and fixed $\alpha = 0.9,\ \gamma = 0.6,\ \lambda_1 = \lambda_2 = -1,\ \nu_1 = \nu_2 = 0.6$ where $N_x, M_y, K_t = 4$

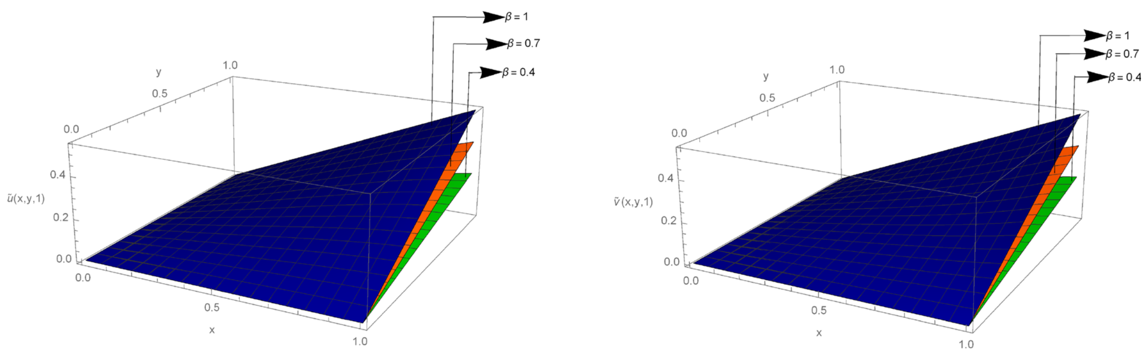

(a) (b)

Fig. 12 Plots of the concentrations of solute $\tilde{u}(x, y, t)$ and $\tilde{v}(x, y, t)$ at $t = 1$ for different values of $\beta = 0.4, 0.7, 1$ and fixed $\alpha = 0.9,\ \gamma = 0.6,\ \lambda_1 = \lambda_2 = -1$, with advection coefficients $\nu_1 = \nu_2 = 0$ where $N_x, M_y, K_t = 4$

The nature of solution profile of Fig. 12 is similar to Fig. 11, but due to the absence of advection terms the concentration of solute is less in each case. It is observed from Fig. 13 that the solute concentrations are lower for the sink terms $(\lambda_1 = -1, \lambda_2 = -1)$ as compared to the source terms $(\lambda = 1, \lambda_2 = 1)$ as well as for the case of conservative system $(\lambda_1 = 0, \lambda_2 = 0)$, when $\alpha = 0.9$, $\beta = 0.8$, $\gamma = 0.7$, $\nu_1 = \nu_2 = 0.6$.

7 Conclusions

In the present scientific contribution a drive has been made to develop a powerful SLGLC numerical scheme to solve the nonlinear coupled 2D-STFRAD equations. The important feature is the error analysis between the results obtained by the proposed numerical approach and the existing results which clearly exhibit the efficiency and effectiveness of the scheme. The another attribute is the showcasing of effects of advection terms and reaction terms on the solution profiles for various space and time derivatives graphically for different particular cases. Important feature is the graphical presentations of the variations of concentration of the concerned model when approaches from fractional order system to the integer order system. The salient feature of the article is the convergence analysis of the proposed scheme while applying on the concerned two dimensional nonlinear coupled model.

The current work creates opportunities for future works to handle the highly non-linear PDEs and also solving wide range of PDEs with variable fractional order derivative as well as integer order derivative.

Author contribution A.: Formal Analysis, Investigation, Methodology, Writing, Original draft. M. C.: Conceptualization, Writing-review and editing, Numerical Simulation. S. D.: Conceptualization, Writing-review

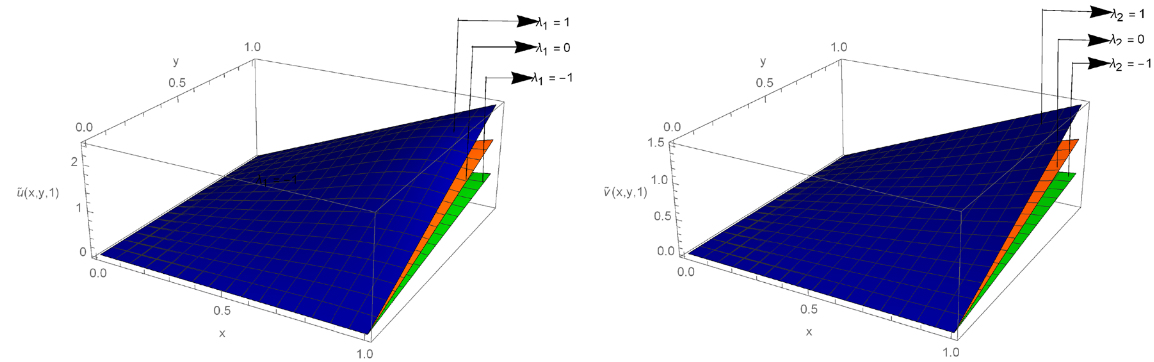

(a) (b)

Fig. 13 Plots of the concentrations of solute $\tilde{u}(x, y, t)$ and $\tilde{v}(x, y, t)$ at $t = 1$ for fixed $\alpha = 0.9,\ \beta = 0.8,\ \gamma = 0.7,\ \nu_1 = \nu_2 = 0.6$ and different values of $\lambda_1 = \lambda_2 = -1, 0, 1$ where $N_x, M_y, K_t = 4$

and editing. H. A.: Writing original draft, Numerical Validation.

Data availability No datasets were generated or analysed during the current study.

Declarations

Conflict of interest The authors declare no competing interests.

Funding Open Access funding enabled and organized by Projekt DEAL.

A Appendix

$$\mathcal{A}_1 = \max\Bigg\{\max\Big|\frac{\partial^{N_x+1}\tilde{u}(x,y,t)}{\partial x^{N_x+1}}\Big|, \max\Big|\frac{\partial^{M_y+1}\tilde{u}(x,y,t)}{\partial y^{M_y+1}}\Big|, \max\Big|\frac{\partial^{K_t+1}\tilde{u}(x,y,t)}{\partial t^{K_t+1}}\Big|, \tag{42}$$

$$\max\Big|\frac{\partial^{N_x+M_y+K_t+3}\tilde{u}(x,y,t)}{\partial x^{N_x+1}\partial y^{M_y+1}\partial t^{K_t+1}}\Big|\Bigg\}, \tag{43}$$

$$\mathcal{A}_2 = \max\Bigg\{\max\Big|\frac{\partial^{N_x+1}\tilde{u}(x,y,t)}{\partial x^{N_x+1}}\Big|, \max\Big|\frac{\partial^{M_y+1}\tilde{v}(x,y,t)}{\partial y^{M_y+1}}\Big|, \max\Big|\frac{\partial^{K_t+1}\tilde{v}(x,y,t)}{\partial t^{K_t+1}}\Big|, \tag{44}$$

$$\max\Big|\frac{\partial^{N_x+M_y+K_t+3}\tilde{v}(x,y,t)}{\partial x^{N_x+1}\partial y^{M_y+1}\partial t^{K_t+1}}\Big|\Bigg\}, \tag{45}$$

$$\mathcal{A}_3 = \max\Bigg\{\max\Big|\frac{\partial^{N_x+1}w_1(x,y,t)}{\partial x^{N_x+1}}\Big|, \max\Big|\frac{\partial^{M_y+1}w_1(x,y,t)}{\partial y^{M_y+1}}\Big|, \max\Big|\frac{\partial^{K_t+1}w_1(x,y,t)}{\partial t^{K_t+1}}\Big|, \tag{46}$$

$$\max\Big|\frac{\partial^{N_x+M_y+K_t+3}w_1(x,y,t)}{\partial x^{N_x+1}\partial y^{M_y+1}\partial t^{K_t+1}}\Big|\Bigg\}, \tag{47}$$

$$\mathcal{A}_4 = \max\Bigg\{\max\Big|\frac{\partial^{N_x+1}w_2(x,y,t)}{\partial x^{N_x+1}}\Big|, \max\Big|\frac{\partial^{M_y+1}w_2(x,y,t)}{\partial y^{M_y+1}}\Big|, \max\Big|\frac{\partial^{K_t+1}w_2(x,y,t)}{\partial t^{K_t+1}}\Big|, \tag{48}$$

$$\max|\frac{\partial^{N_x+M_y+K_t+3}w_2(x,y,t)}{\partial x^{N_x+1}\partial y^{M_y+1}\partial t^{K_t+1}}|\Big\}, \tag{49}$$

$$\mathcal{A}_5=\max\Big\{\max|\frac{\partial^{N_x+1}w_3(x,y,t)}{\partial x^{N_x+1}}|,\max|\frac{\partial^{M_y+1}w_3(x,y,t)}{\partial y^{M_y+1}}|,\max|\frac{\partial^{K_t+1}w_3(x,y,t)}{\partial t^{K_t+1}}|, \tag{50}$$

$$\max|\frac{\partial^{N_x+M_y+K_t+3}w_3(x,y,t)}{\partial x^{N_x+1}\partial y^{M_y+1}\partial t^{K_t+1}}|\Big\}, \tag{51}$$

$$\mathcal{A}_6=\max\Big\{\max|\frac{\partial^{N_x+1}w_4(x,y,t)}{\partial x^{N_x+1}}|,\max|\frac{\partial^{M_y+1}w_4(x,y,t)}{\partial y^{M_y+1}}|,\max|\frac{\partial^{K_t+1}w_4(x,y,t)}{\partial t^{K_t+1}}|, \tag{52}$$

$$\max|\frac{\partial^{N_x+M_y+K_t+3}w_4(x,y,t)}{\partial x^{N_x+1}\partial y^{M_y+1}\partial t^{K_t+1}}|\Big\}, \tag{53}$$

$$\mathcal{A}_7=\max\Big\{\max|\frac{\partial^{N_x+1}w_5(x,y,t)}{\partial x^{N_x+1}}|,\max|\frac{\partial^{M_y+1}w_5(x,y,t)}{\partial y^{M_y+1}}|,\max|\frac{\partial^{K_t+1}w_5(x,y,t)}{\partial t^{K_t+1}}|, \tag{54}$$

$$\max|\frac{\partial^{N_x+M_y+K_t+3}w_5(x,y,t)}{\partial x^{N_x+1}\partial y^{M_y+1}\partial t^{K_t+1}}|\Big\}, \tag{55}$$

$$\mathcal{A}_8=\max\Big\{\max|\frac{\partial^{N_x+1}w_6(x,y,t)}{\partial x^{N_x+1}}|,\max|\frac{\partial^{M_y+1}w_6(x,y,t)}{\partial y^{M_y+1}}|,\max|\frac{\partial^{K_t+1}w_6(x,y,t)}{\partial t^{K_t+1}}|, \tag{56}$$

$$\max|\frac{\partial^{N_x+M_y+K_t+3}w_6(x,y,t)}{\partial x^{N_x+1}\partial y^{M_y+1}\partial t^{K_t+1}}|\Big\}, \tag{57}$$

$$\mathcal{A}_9=\max\Big\{\max|\frac{\partial^{N_x+1}w_7(x,y,t)}{\partial x^{N_x+1}}|,\max|\frac{\partial^{M_y+1}w_7(x,y,t)}{\partial y^{M_y+1}}|,\max|\frac{\partial^{K_t+1}w_7(x,y,t)}{\partial t^{K_t+1}}|, \tag{58}$$

$$\max|\frac{\partial^{N_x+M_y+K_t+3}w_7(x,y,t)}{\partial x^{N_x+1}\partial y^{M_y+1}\partial t^{K_t+1}}|\Big\}, \tag{59}$$

$$\mathcal{A}_{10}=\max\Big\{\max|\frac{\partial^{N_x+1}w_8(x,y,t)}{\partial x^{N_x+1}}|,\max|\frac{\partial^{M_y+1}w_8(x,y,t)}{\partial y^{M_y+1}}|,\max|\frac{\partial^{K_t+1}w_8(x,y,t)}{\partial t^{K_t+1}}|, \tag{60}$$

$$\max|\frac{\partial^{N_x+M_y+K_t+3}w_8(x,y,t)}{\partial x^{N_x+1}\partial y^{M_y+1}\partial t^{K_t+1}}|\Big\}, \tag{61}$$

$$\mathcal{A}_{11}=\max\Big\{\max|\frac{\partial^{N_x+1}g_1(x,y,t)}{\partial x^{N_x+1}}|,\max|\frac{\partial^{M_y+1}g_1(x,y,t)}{\partial y^{M_y+1}}|,\max|\frac{\partial^{K_t+1}g_1(x,y,t)}{\partial t^{K_t+1}}|, \tag{62}$$

$$\max|\frac{\partial^{N_x+M_y+K_t+3}g_1(x,y,t)}{\partial x^{N_x+1}\partial y^{M_y+1}\partial t^{K_t+1}}|\Big\}, \tag{63}$$

$$\mathcal{A}_{12}=\max\Big\{\max|\frac{\partial^{N_x+1}g_2(x,y,t)}{\partial x^{N_x+1}}|,\max|\frac{\partial^{M_y+1}g_2(x,y,t)}{\partial y^{M_y+1}}|,\max|\frac{\partial^{K_t+1}g_2(x,y,t)}{\partial t^{K_t+1}}|, \tag{64}$$

$$\max|\frac{\partial^{N_x+M_y+K_t+3}g_2(x,y,t)}{\partial x^{N_x+1}\partial y^{M_y+1}\partial t^{K_t+1}}|\Big\}, \tag{65}$$

$$\mathcal{A}_{13}=\max\Big\{\max|\frac{\partial^{N_x+1}\tilde{u}^2(x,y,t)}{\partial x^{N_x+1}}|,\max|\frac{\partial^{M_y+1}\tilde{u}^2(x,y,t)}{\partial y^{M_y+1}}|,\max|\frac{\partial^{K_t+1}\tilde{u}^2(x,y,t)}{\partial t^{K_t+1}}|, \tag{66}$$

$$\max|\frac{\partial^{N_x+M_y+K_t+3}\tilde{u}^2(x,y,t)}{\partial x^{N_x+1}\partial y^{M_y+1}\partial t^{K_t+1}}|\Big\}, \tag{67}$$

$$\mathcal{A}_{14}=\max\Big\{\max|\frac{\partial^{N_x+1}\tilde{u}\tilde{v}(x,y,t)}{\partial x^{N_x+1}}|,\max|\frac{\partial^{M_y+1}\tilde{u}\tilde{v}(x,y,t)}{\partial y^{M_y+1}}|,\max|\frac{\partial^{K_t+1}\tilde{u}\tilde{v}(x,y,t)}{\partial t^{K_t+1}}|, \tag{68}$$

$$\max|\frac{\partial^{N_x+M_y+K_t+3}\tilde{u}\tilde{v}(x,y,t)}{\partial x^{N_x+1}\partial y^{M_y+1}\partial t^{K_t+1}}|\Big\}, \tag{69}$$

$$\mathcal{A}_{15} = \max\left\{\max\left|\frac{\partial^{N_x+1}\tilde{v}^2(x,y,t)}{\partial x^{N_x+1}}\right|, \max\left|\frac{\partial^{M_y+1}\tilde{v}^2(x,y,t)}{\partial y^{M_y+1}}\right|, \max\left|\frac{\partial^{K_t+1}\tilde{v}^2(x,y,t)}{\partial t^{K_t+1}}\right|,\right. \tag{70}$$

$$\left.\max\left|\frac{\partial^{N_x+M_y+K_t+3}\tilde{v}^2(x,y,t)}{\partial x^{N_x+1}\partial y^{M_y+1}\partial t^{K_t+1}}\right|\right\},\ at\ (x,y)\in[0,1]\times[0,1]\,,t\in[0,1]\,. \tag{71}$$

References

1. Biswas, C., Das, S., Singh, A., Altenbach, H.: Solution of variable-order partial integro-differential equation using Legendre wavelet approximation and operational matrices. ZAMM-J. Appl. Math. Mechanics/Zeitschrift für Angewandte Mathematik und Mechanik **103**(2), 202200222 (2023). https://doi.org/10.1002/zamm.202200222
2. Bear, J.: Dynamics of fluids in porous media. Cour. Corp., Chelmsf. (2013). https://doi.org/10.1097/00010694-197508000-00022
3. Deng, Y., Liu, C.: Mathematical model of two-phase fluid nonlinear flow in low-permeability porous media with applications. Appl. Math. Mech. **24**, 1184–1193 (2003). https://doi.org/10.1007/BF02438107
4. Singh, A., Das, S.: Study and analysis of spatial-time nonlinear fractional-order reaction-advection-diffusion equation. J. Porous Med. **22**(7), 787–798 (2019). https://doi.org/10.1615/JPorMedia.2019025907
5. Jaiswal, S., Chopra, M., Ong, S.H., Das, S.: Numerical solution of one-dimensional finite solute transport system with first type source boundary condition. Int. J. Appl. Comput. Math. **3**, 3035–3045 (2017). https://doi.org/10.1007/s40819-016-0280-6
6. Yang, Q., Turner, I., Liu, F., Ilić, M.: Novel numerical methods for solving the time-space fractional diffusion equation in two dimensions. SIAM J. Sci. Comput. **33**(3), 1159–1180 (2011). https://doi.org/10.1137/100800634
7. Anjuman, Leung, A.Y., Das, S.: Two-dimensional time-fractional nonlinear drift reaction-diffusion equation arising in electrical field. Fractal Fract. **8**(8), 456 (2024). https://doi.org/10.3390/fractalfract8080456
8. Bakkyaraj, T.: Lie symmetry analysis of system of nonlinear fractional partial differential equations with Caputo fractional derivative. Eur. Phys. J. Plus **135**(1), 126 (2020). https://doi.org/10.1140/epjp/s13360-020-00170-9
9. Li, C., Qian, D., Chen, Y.: On Riemann-Liouville and Caputo derivatives. Discret. Dyn. Nat. Soc. **2011**(1), 562494 (2011). https://doi.org/10.1155/2011/562494
10. Abdelouahab, M.S., Hamri, N.E.: The Grünwald-Letnikov fractional-order derivative with fixed memory length. Mediterr. J. Math. **13**(2), 557–572 (2016). https://doi.org/10.1007/s00009-015-0525-3
11. Osler, T.J.: The fractional derivative of a composite function. SIAM J. Math. Anal. **1**(2), 288–293 (1970). https://doi.org/10.1137/0501026
12. Li, C., Cai, M.: Theory and numerical approximations of fractional integrals and derivatives. SIAM, Philadelphia. (2020). https://doi.org/10.1137/1.9781611975888
13. Atangana, A., Owolabi, K.M.: New numerical approach for fractional differential equations. Math. Model. Nat. Phenom. **13**(1), 3 (2018). https://doi.org/10.1051/mmnp/2021039
14. Agarwal, P., Ramadan, M.A., Rageh, A.A.M., Hadhoud, A.R.: A fractional-order mathematical model for analyzing the pandemic trend of COVID-19. Math. Methods Appl. Sci. **45**(8), 4625–4642 (2022). https://doi.org/10.1002/mma.8057
15. Hadhoud, A.R., Agarwal, P., Rageh, A.A.M.: Numerical treatments of the nonlinear coupled time-fractional Schrödinger equations. Math. Methods Appl. Sci. **45**(11), 7119–7143 (2022). https://doi.org/10.1002/mma.8228
16. Hamid, M., Usman, M., Tian, Z.: Computational analysis for fractional characterization of coupled convection-diffusion equations arising in MHD flows. Appl. Math. Mech. **44**(4), 669–692 (2023). https://doi.org/10.1007/s10483-023-2970-6
17. Liu, Y., Zhao, Z., Zhang, Y., Pang, J.: Approximate solutions to fractional differential equations. Appl. Math. Mech. **44**(10), 1791–1802 (2023). https://doi.org/10.1007/s10483-023-3041-9
18. Atanackovic, T.M., Pilipovic, S., Zorica, D.: Distributed-order fractional wave equation on a finite domain: creep and forced oscillations of a rod. Continuum Mech. Thermodyn. **23**, 305–318 (2011). https://doi.org/10.1007/s00161-010-0177-2
19. Lion, A.: On the thermodynamics of fractional damping elements. Continuum Mech. Thermodyn. **9**, 83–96 (1997). https://doi.org/10.1007/s001610050057
20. Povstenko, Y.: Fractional thermoelasticity, 2nd edn., Cham (2024). https://doi.org/10.1007/978-3-031-64587-7
21. Bhrawy, A.H.: A new Legendre collocation method for solving a two-dimensional fractional diffusion equation. Abstr. Appl. Anal. **2014**(1), 636191 (2014). https://doi.org/10.1155/2014/636191
22. Zhou, F., Xu, X.: The third kind Chebyshev wavelets collocation method for solving the time-fractional convection diffusion equations with variable coefficients. Appl. Math. Comput. **280**, 11–29 (2016). https://doi.org/10.1016/j.amc.2016.01.029
23. Reddy, J.N.: Introduction to the finite element method. McGraw-Hill Education, New York (2019)
24. Strikwerda, J.C.: Finite Difference Schemes and Partial Differential Equations, 2nd edn. SIAM, Philadelphia (2004). https://doi.org/10.1137/1.9780898717938
25. Biswas, C., Singh, A., Chopra, M., Das, S.: Study of fractional-order reaction-advection-diffusion equation using neural network method. Math. Comput. Simul. **208**, 15–27 (2023). https://doi.org/10.1016/j.matcom.2022.12.032
26. Abdelkawy, M.A., Alqahtani, R.T.: Shifted Jacobi collocation method for solving multi-dimensional fractional Stokes' first problem for a heated generalized second grade fluid. Adv. Differ. Equ. **2016**(1), 114 (2016). https://doi.org/10.1186/s13662-016-0845-z
27. Ren, R.-F., Li, H.-B., Jiang, W., Song, M.-Y.: An efficient Chebyshev-tau method for solving the space fractional diffusion equations. Appl. Math. Comput. **224**, 259–267 (2013). https://doi.org/10.1016/j.amc.2013.08.073
28. Atta, A., Abd-Elhameed, W., Moatimid, G., Youssri, Y.: Advanced shifted sixth-kind Chebyshev tau approach for solving linear one-dimensional hyperbolic telegraph type problem. Math. Sci. **17**(4), 415–429 (2023). https://doi.org/10.1007/s40096-022-00460-6

29. Wang, H., Basu, T.S.: A fast finite difference method for two-dimensional space-fractional diffusion equations. SIAM J. Sci. Comput. **34**(5), 2444–2458 (2012). https://doi.org/10.1137/12086491X
30. Saffarian, M., Mohebbi, A.: Finite difference/spectral element method for one and two-dimensional Riesz space fractional advection-dispersion equations. Math. Comput. Simul. **193**, 348–370 (2022). https://doi.org/10.1016/j.matcom.2021.10.020
31. Owolabi, K.M.: Numerical approach to chaotic pattern formation in diffusive predator-prey system with Caputo fractional operator. Numer. Methods Partial Differ. Equ. **37**(1), 131–151 (2021). https://doi.org/10.1002/num.22522
32. Hadhoud, A.R., Srivastava, H.M., Rageh, A.A.M.: Non-polynomial B-spline and shifted Jacobi spectral collocation techniques to solve time-fractional nonlinear coupled Burgers' equations numerically. Adv. Diff. Equ. **2021**(1), 439 (2021). https://doi.org/10.1186/s13662-021-03604-5
33. Dişibüyük, Ç., Goldman, R.: A unified approach to non-polynomial B-spline curves based on a novel variant of the polar form. Calcolo **53**, 751–781 (2016). https://doi.org/10.1007/s10092-015-0172-x
34. Bhrawy, A.H., Alzaidy, J.F., Abdelkawy, M.A., Biswas, A.: Jacobi spectral collocation approximation for multi-dimensional time-fractional schrödinger equations. Nonlinear Dyn. **84**, 1553–1567 (2016). https://doi.org/10.1007/s11071-015-2588-x
35. Che, H., Wang, Y.-L., Li, Z.-Y.: Novel patterns in a class of fractional reaction-diffusion models with the Riesz fractional derivative. Math. Comput. Simul. **202**, 149–163 (2022). https://doi.org/10.1016/j.matcom.2022.05.037
36. Huang, J., Zhang, J., Arshad, S., Tang, Y.: A numerical method for two-dimensional multi-term time-space fractional nonlinear diffusion-wave equations. Appl. Numer. Math. **159**, 159–173 (2021). https://doi.org/10.1016/j.apnum.2020.09.003
37. Li, D., Qiao, Z., Tang, T.: Characterizing the stabilization size for semi-implicit Fourier-spectral method to phase field equations. SIAM J. Numer. Anal. **54**(3), 1653–1681 (2016). https://doi.org/10.1137/140993193
38. El-Sayed, A.A., Agarwal, P.: Numerical solution of multiterm variable-order fractional differential equations via shifted Legendre polynomials. Math. Methods Appl. Sci. **42**(11), 3978–3991 (2019). https://doi.org/10.1002/mma.5627
39. Bhrawy, A., Alghamdi, M.: A shifted Jacobi-Gauss collocation scheme for solving fractional neutral functional-differential equations. Adv. Math. Phys. **2014**(1), 595848 (2014). https://doi.org/10.1155/2014/595848
40. Bhrawy, A.H., Zaky, M.A., Alzaidy, J.F.: Two shifted Jacobi-Gauss collocation schemes for solving two-dimensional variable-order fractional Rayleigh-Stokes problem. Adv. Difference Equ. **2016**(1), 1–17 (2016). https://doi.org/10.1186/s13662-016-0998-9
41. Wang, Y., Chen, Y.: Shifted Legendre polynomials algorithm used for the dynamic analysis of viscoelastic pipes conveying fluid with variable fractional order model. Appl. Math. Model. **81**, 159–176 (2020). https://doi.org/10.1016/j.apm.2019.12.011
42. Hadhoud, A.R., Rageh, A.A.M., Agarwal, P.: Numerical method for solving two-dimensional of the space and space-time fractional coupled reaction-diffusion equations. Math. Methods Appl. Sci. **46**(5), 6054–6076 (2023). https://doi.org/10.1002/mma.8891
43. Hildebrand, F.B.: Introduction to numerical analysis, 2nd edn. Dover Books on Advanced Mathematics. Dover Publications Inc., (1987)
44. Shen, S., Liu, F., Chen, J., Turner, I., Anh, V.: Numerical techniques for the variable order time fractional diffusion equation. Appl. Math. Comput. **218**(22), 10861–10870 (2012). https://doi.org/10.1016/j.amc.2012.04.047
45. Heydari, M.H., Hosseininia, M., Baleanu, D.: A computational approach based on the fractional Euler functions and Chebyshev cardinal functions for distributed-order time fractional 2D diffusion equation. Alex. Eng. J. **67**, 643–653 (2023). https://doi.org/10.1016/j.aej.2022.12.065